

Core Cosmology Library: Precision Cosmological Predictions for LSST

Husni Almoubayyed,¹ David Alonso,² Jonathan Blazek,^{3,4} Philip Bull,^{5,6}
 Jean-Éric Campagne,⁷ N. Elisa Chisari,² Alex Drlica-Wagner,⁸ Zilong Du,⁹
 Tim Eifler,^{10,11} John Ellison,⁹ Renée Hlozek,¹² Mustapha Ishak,¹³ Shahab Joudaki,²
 Matthew Kirby,¹⁴ David Kirkby,¹⁵ Elisabeth Krause,^{10,16} Francois Lanusse,¹
 C. Danielle Leonard,¹ Christiane S. Lorenz,² Phil Marshall,¹⁷ Thomas McClintock,¹⁴
 Sean McLaughlin,¹⁸ Alexander Mead,¹⁹ Jérémy Neveu,⁷ Stéphane Plaszczyński,⁷
 Javier Sanchez,¹⁵ Sukhdeep Singh,¹ Anže Slosar,²⁰ Tilman Tröster,²¹
 Antonio Villarreal,²² Michal Vrástl,²³ and Joe Zuntz²¹
 (LSST Dark Energy Science Collaboration)

¹McWilliams Center for Cosmology, Department of Physics, Carnegie Mellon University, Pittsburgh, PA 15213, USA

²Department of Physics, University of Oxford, Denys Wilkinson Building, Keble Road, Oxford OX1 3RH, United Kingdom

³Center for Cosmology and Astroparticle Physics, Ohio State, Columbus, OH 43210, USA

⁴Laboratory of Astrophysics, École Polytechnique Fédérale de Lausanne (EPFL), Observatoire de Sauverny, 1290 Versoix, Switzerland

⁵California Institute of Technology, Pasadena, CA 91125, USA

⁶Jet Propulsion Laboratory, California Institute of Technology, 4800 Oak Grove Drive, Pasadena, California, USA

⁷Laboratoire de l'Accélérateur Linéaire, Université Paris-Sud, CNRS/IN2P3, Université Paris-Saclay, Orsay, France

⁸Fermi National Accelerator Laboratory, P. O. Box 500, Batavia, IL 60510, USA

⁹Department of Physics and Astronomy, University of California, Riverside, CA 92521, USA

¹⁰Steward Observatory/Department of Astronomy, University of Arizona, 933 North Cherry Avenue, Tucson, AZ 85721, USA

¹¹Jet Propulsion Laboratory, California Institute of Technology, Pasadena, CA 91109, USA

¹²Dunlap Institute for Astronomy and Astrophysics & Department of Astronomy and Astrophysics, University of Toronto, ON M5S 3H4

¹³Department of Physics, The University of Texas at Dallas, Richardson, TX 75083, USA

¹⁴University of Arizona, Tucson, AZ 85721, USA

¹⁵Department of Physics and Astronomy, University of California, Irvine, CA 92697, USA

¹⁶Kavli Institute for Particle Astrophysics and Cosmology, Stanford, CA 94305-4085, USA

¹⁷SLAC National Accelerator Laboratory, Menlo Park, CA 94025, USA

¹⁸Stanford University, Stanford, CA, 94305, USA

¹⁹Department of Physics and Astronomy, University of British Columbia, 6224 Agricultural Road, Vancouver, BC V6T 1Z1, Canada

²⁰Brookhaven National Laboratory, Physics Department, Upton, NY 11973, USA

²¹Institute for Astronomy, Royal Observatory Edinburgh, Edinburgh EH9 3HJ, UK

²²Department of Physics and Astronomy, University of Pittsburgh, Pittsburgh PA 15260

²³Institute of Physics CAS, Prague, 182 21, CZ

The Core Cosmology Library (CCL) provides routines to compute basic cosmological observables with validated numerical accuracy. These routines have been validated to an accuracy level, documented here, against the results of independent implementations. In the current version, predictions are provided for distances and background quantities, angular auto- and cross-spectra of cosmic shear, galaxy-galaxy lensing, intrinsic alignments and clustering, halo bias and the halo mass function. CCL uses different schemes to obtain the matter power spectrum, including analytical, phenomenological and other schemes calibrated through simulations. Fiducial specifications for the expected LSST galaxy distributions and

clustering bias are also included, together with the capability of computing redshift distributions for a user-defined photometric redshift model. CCL is written in C, with a Python interface. In this note, we explain the functionality of the publicly released (CCL v1) library.

Contents

1. Introduction	6
2. Installation	6
2.1. General installation	6
2.2. Dependencies	7
2.3. Installing the dependencies	7
2.4. Compile and install the C library	8
2.5. Install the pyccl Python module	10
2.6. Known installation issues	11
2.7. Compiling against an external version of CLASS	12
2.8. Creating a Docker Image	12
3. Documentation	13
4. Functionality	13
4.1. Physical constants	13
4.2. Supported cosmological models	13
4.3. Creating a cosmology	14
4.4. Distances	17
4.5. Density parameter functions	18
4.6. Functions of the physical density	19

4.7. Growth function	20
4.8. Matter power spectrum	20
4.8.1. BBKS	21
4.8.2. Eisenstein and Hu	21
4.8.3. CLASS	21
4.8.4. Cosmic emulator	22
4.8.5. Impact of baryons	24
4.8.6. Spline parameters & the INI file	24
4.8.7. Extrapolation for the nonlinear power spectrum	28
4.8.8. Extrapolation for the linear power spectrum	29
4.8.9. Wishlist for the future	30
4.8.10. Normalization of the power spectrum	30
4.9. Angular power spectra	31
4.9.1. Exact expressions	31
4.9.2. The Limber approximation	33
4.9.3. Beyond limber	34
4.10. Correlation functions	37
4.11. Halo mass & halo bias functions	38
4.12. Halo model	40
4.13. Photo- z implementation	42
4.14. LSST Specifications	43

	5
5. Tests and validation	44
6. Examples for C implementation	51
7. Python example	51
8. Technical notes on how the Python wrapper is implemented	53
9. Future functionality to be included	54
10. Feedback	55
11. Citing & using CCL	55
12. License	56

1. Introduction

In preparation for constraining cosmology with the Large Synoptic Survey Telescope (LSST), it is necessary to be able to produce rigorous theoretical predictions for the cosmological quantities that will be measured. The Core Cosmology Library¹ (CCL) aims to provide, in one library, a way of making predictions that are validated to a well-documented numerical accuracy, for the purpose of constraining cosmology with LSST. By constructing a cosmology library specifically with LSST in mind, it is possible to ensure that it is flexible, adaptable, and validated for all cases of interest, as well as user-friendly and appropriate for the needs of all working groups.

The Core Cosmology Library is written in C and incorporates the CLASS code (Blas et al. 2011) to provide predictions for the matter power spectrum. It also incorporates emulated power spectra from the cosmic emulator of Lawrence et al. (2017).² A Python wrapper is also provided for ease of use.

This note describes how to install CCL (Section 2), how CCL is documented (Section 3), its functionality (Section 4), the relevant unit tests (Section 5), directions for finding a CCL example (Section 6) in C, a Python example and technical details on the Python wrapper (Section 7), details on the Python implementation (Section 8), future plans (Section 9), means to contact the developers (Section 10), instructions on how to cite CCL (and CLASS, Section 11), and the license under which CCL is released (Section 12).

2. Installation

2.1. General installation

CCL is available as a Python package through PyPi. To install, simply run:

```
$ pip install pyccl
```

This should work as long as CMake is installed on your system (if it isn't, follow the detailed instructions below).

¹ <https://github.com/LSSTDESC/CCL>

² Future versions of the library will incorporate other power-spectrum libraries and methods.

CCL comes in two forms: a C library and a Python module. These components can be installed independently of each other, instructions are provided below.

For developers: Note that the installation procedure for development workflow is different than stated here. Detailed instructions are provided in the README.md file in the main CCL directory.

2.2. Dependencies

CCL requires the following software and libraries

- GNU Scientific Library GSL,³ GSL-2.1 or higher.
- FFTW⁴ version 3.1 or above is required for computation of correlation functions.
- FFTlog⁵ is provided within CCL, with minor modifications.
- The C library associated to the CLASS code. (Note that, if you want to use your own version of CLASS, you should follow the steps described in Section 2.7 below.)
- Angpow (Campagne et al. 2017) for fast computation of angular power spectra beyond the Limber approximation⁶.

In addition, the build system for CCL requires

- The SWIG⁷ Python wrapper.
- CMake⁸ version 3.2 or above. This is the only requirement that needs to be manually installed (see below).

2.3. Installing the dependencies

It is preferable to install GSL and FFTW on your system before building CCL, but only necessary if you want to properly install the C library, otherwise CMake will

³ <https://www.gnu.org/software/gsl/>

⁴ <http://www.fftw.org>

⁵ <http://casa.colorado.edu/~ajsh/FFTLog/> and <https://github.com/slosar/FFTLog>

⁶ <https://gitlab.in2p3.fr/campagne/AngPow>

⁷ <http://www.swig.org/>

⁸ <https://cmake.org/>

automatically download and build the missing requirements in order to compile CCL.

For CMake, you can follow this set of instructions. On Ubuntu:

```
$ sudo apt-get install cmake
```

On MacOS X:

- Install using a DMG package from this download page: <https://cmake.org/download/>.
- Or install using a package manager (e.g., brew⁹), MacPorts¹⁰, Fink¹¹). For instance, with brew:

```
$ brew install cmake
```

To install all the dependencies at once, and avoid having CMake recompiling them, for instance on Ubuntu:

```
$ sudo apt-get install cmake swig libgsl-dev libfftw3-dev
```

2.4. Compile and install the C library

To download the latest version of CCL:

```
$ git clone https://github.com/LSSTDESC/CCL.git
$ cd CCL
```

or download and extract the latest stable release from <https://github.com/LSSTDESC/CCL/releases>. Then, from the base CCL directory run:

```
$ mkdir build && cd build
$ cmake ..
```

⁹ <https://brew.sh/>

¹⁰ <https://www.macports.org/>

¹¹ <http://www.finkproject.org/>

This will run the configuration script, try to detect the required dependencies on your machine and generate a Makefile. Once CMake has been configured, to build and install the library simply run for the `build` directory:

```
$ make
$ make install
```

Often admin privileges will be needed to install the library. If you have those just type:

```
$ sudo make install
```

Note: This is the default install procedure, but depending on your system you might want to customize the install process. Here are a few common configuration options:

- **C compiler:** In case you have several C compilers on your machine, you will probably need to specify which one to use to CMake by setting the environment `CC` like so, ****before**** running CMake:

```
$ export CC=gcc
```

- **Install directory:** By default, CMake will try to install CCL in `/usr/local`, if you would like to instead install CCL in a user-defined directory (for instance if you don't have admin privileges), you can specify it to CMake by running instead the following command:

```
$ cmake -DCMAKE_INSTALL_PREFIX=/path/to/install ..
```

This will instruct CMake to install CCL in the following folders:
`/path/to/install/include,/path/to/install/share,/path/to/install/lib.`

Depending on where you install CCL you might need to add the installation path to your `PATH` and `LD_LIBRARY_PATH` environment variables. In the default case, it will look like:

```
$ export LD_LIBRARY_PATH=$LD_LIBRARY_PATH:/usr/local/lib
$ export PATH=$PATH:/usr/local/bin
```

To make sure that everything is working properly, you can run all unit tests after installation by running **from the root CCL directory**:

```
$ ./build/check_ccl
```

Assuming that the tests pass, you have successfully installed CCL!

If you ever need to uninstall CCL, run the following from the `build` directory:

```
$ make uninstall
```

You may need to prepend a `sudo` if you installed CCL in a protected folder.

2.5. Install the `pyccl` Python module

CCL also comes with a Python wrapper, called `pyccl`, which can be built and installed regardless of whether you install the C library. For convenience, we provide a PyPi hosted package which can be installed simply by running:

```
$ pip install pyccl
```

(Append `--user` for single user install.) This only assumes that `CMake` is available on your system, you don't need to download the source yourself.

You can also build and install `pyccl` from the CCL source, again **without necessarily installing the C library**. Download the latest version of CCL:

```
$ git clone https://github.com/LSSTDESC/CCL.git
$ cd CCL
```

or download and extract the latest stable release from <https://github.com/LSSTDESC/CCL/releases>. And from the root CCL folder, simply run:

```
$ python setup.py install # append --user for single user install
```

The `pyccl` module will be installed into a sensible location in your `PYTHONPATH`, and so should be picked up automatically by your Python interpreter. You can then simply import the module using `import pyccl`.

You can quickly check whether `pyccl` has been installed correctly by running `python -c "import pyccl"` and checking that no errors are returned.

For a more in-depth test to make sure everything is working, run from the root CCL directory:

```
$ python setup.py test
```

This will run the embedded unit tests (may take a few minutes).

Whatever the install method, you can always uninstall the python wrapper by running:

```
$ pip uninstall pyccl
```

For quick introduction to CCL in Python, take a look at notebooks in `examples/`.

2.6. Known installation issues

In case you have several C compilers on your system, CMake may not default to the one you want to use. You can specify which C compiler will be used to compile CCL by setting the `CC` environment variable **before** calling any `cmake` or `python setup.py` commands:

```
$ export CC=gcc
```

If upon running the C tests you get an error from `CLASS` saying it cannot find the file `sBBN_2017.dat`, it means that the `CLASS` parameter files are not properly installed on your system. Make sure you have indeed installed the C library by running:

```
$ make install
```

from the `CCL/build` directory.

Other known installation issues are documented in the CCL wiki within the repository.

2.7. Compiling against an external version of CLASS

The default installation procedure for CCL implies automatically downloading and installing a tagged version of CLASS. Optionally, you can also link CCL against a different version of CLASS. This is useful if you want to use a modified version of CLASS, or a different or more up-to-date version of the standard CLASS.

To compile CCL with an external version of CLASS, just run the following CMake command at the first configuration step of the install (from the `build` directory, make sure it is empty to get a clean configuration):

```
$ cmake -DEXTERNAL_CLASS_PATH=/path/to/class ..
```

the rest of the build process should be the same.

2.8. Creating a Docker Image

The Dockerfile to generate a Docker image is included in the CCL repository as `Dockerfile`. This can be used to create an image that Docker can spool up as a virtual machine, allowing you to utilize CCL on any infrastructure with minimal hassle. The details of Docker and the installation process can be found at <https://www.docker.com/>. Once Docker is installed, it is a simple process to create an image. In a terminal of your choosing (with Docker running), type the command `docker build -t ccl .` in the CCL directory.

The resulting Docker image has two primary functionalities. The first is a CMD that will open Jupyter notebook tied to a port on your local machine. This can be used with the following run command: `docker run -p 8888:8888 ccl`. You can then access the notebook in the browser of your choice at `localhost:8888`. The second is to access the bash itself, which can be done using `docker run -it ccl bash`.

This Dockerfile currently contains all installed C libraries and the Python wrapper. It currently uses `continuumio/anaconda` as the base image and supports `ipython` and Jupyter notebook. There should be minimal slowdown due to the virtualization.

3. Documentation

CCL has basic `doxygen`¹² documentation for its C routines. This can be found in the directory `doc/html` within the CCL repository by opening the `index.html` file in your browser. The `python` routines are documented in situ; you can view the documentation for a function by calling `help(function_name)` from within `python`. A Readthedocs interface is also available, where you can browse the documentation, at: <https://readthedocs.org/projects/ccl/>.

4. Functionality

4.1. Physical constants

We have performed a comparison of the physical constants used in CCL and included dependencies and external sources. See Table 1 for absolute fractional differences of the constants between these sources. Our final choice of constants for CCL mainly relies on CODATA 2014 (Mohr et al. 2016) in as much as possible, except for M_{\odot} , where we adopt the IAU 2015 value (Mamajek et al. 2015), and for the conversion between parsec and meters, where we take the PDG 2013¹³ value. Notice that NIST¹⁴ adopts the CODATA 2014 values.

Notice there are some inconsistencies with the constants adopted by CLASS. This includes the value of the gravitational constant, the Boltzmann constant, the Planck constant, the speed of light, and the electron charge. Also, the value of ρ_c is derived from other constants, while PDG 2013 fixes it to a given value (this is the reason there is only one entry for that column).

After comparison between the physical constants used in CCL and those of the sources mentioned above, we have found better than 0.01% agreement for all constants of interest except for the gravitational constant and the value of the solar mass.

4.2. Supported cosmological models

¹² <http://www.stack.nl/~dimitri/doxygen/>

¹³ <http://pdg.lbl.gov/2013/>

¹⁴ <https://physics.nist.gov/cuu/Constants/index.html>

Table 1. Absolute fractional differences between different constants as tabulated in the sources listed below. Entries marked with zero indicate that this is the value adopted by CCL.

	G_{Newt}	k_b	σ_{SB}	h	c	eV	ρ_c	M_\odot	pc
PDG 2013	3e-05	2.1e-07	1.1e-06	7e-08	0.0e+00	3.5e-08	8.8e-10	2.2e-05	0.0e+00
NIST	0.0e+00	0.0e+00	0.0e+00	0.0e+00	0.0e+00	0.0e+00	–	–	–
GSL 2.4	1.6e-04	1.1e-06	5.8e-06	6e-09	1.5e-06	2.1e-06	–	2.2e-04	7.8e-07
CLASS	3.0e-05	1.4e-06	–	1.6e-07	0.0e+00	8.4e-08	–	–	1.2e-09
CODATA 2014	0.0e+00	0.0e+00	0.0e+00	0.0e+00	0.0e+00	0.0e+00	–	–	–
IAU 2015	0.0e+00	–	–	–	–	–	–	0.0e+00	–

Ultimately, CCL plans to incorporate theoretical predictions for all cosmological models of interest to LSST. Currently, the following families of models are supported:

- Flat Λ CDM
- wCDM and the CPL model ($w_0 + w_a$, [Chevallier & Polarski 2001](#) and [Linder 2003](#))
- Non-zero curvature (K)
- All of the above, plus an arbitrary, user-defined modified growth function (see description in Section [4.7](#))
- Massive neutrinos, in combination with any of the above.

CCL also provides support for modeling the impact of baryons on the matter power spectrum, as described in Sec. [4.8.5](#). Not all features of CCL are available for all models. For a guide to which predictions are available for each model, see Table [2](#). Note that if users install their own version of CLASS, CCL can then make predictions for a more extended set of cosmologies. Users should take care to understand the validity of the CCL assumptions for their own models.

In its default configuration, CCL adopts the nonlinear matter power spectrum from CLASS through the Halofit implementation and the Tinker mass function for cluster number counts.

4.3. Creating a cosmology

To use CCL, the first step is to create a `ccl_cosmology` structure, containing all of the information required to compute cosmological observables. A `ccl_cosmology`

Table 2. Cosmologies implemented in CCL and observables supported in each of them. Note that the only reason why angular power spectra appear not to be supported in non-flat cosmologies is that the hyperspherical Bessel functions are currently not implemented, although their impact is fairly limited. Likewise, number counts power spectra are strictly not supported in the presence of massive neutrino cosmologies due to the scale-dependent growth rate that affects the redshift-space distortions term, even though the impact of this is also small for wide tomographic bins. The halo model can make matter power spectrum predictions for all cosmologies, but should not be used for massive neutrino models because the current version does not distinguish between the cold matter, relevant for clustering, and all matter. Finally, notice that in addition CCL can make predictions for the growth of perturbations for some modified gravity models through a user defined $\Delta f(a)$, and that other extensions are supported via integration of external modified gravity codes.

Observable/Model	flat Λ CDM	Λ CDM+K	Λ CDM + m_ν	w CDM
Distances	✓	✓	✓	✓
Growth	✓	✓	X	✓
$P_m(k, z)$	✓	✓	✓	✓
Halo Mass Function	✓	✓	X	✓
C_l , number counts	✓	X	X	✓
C_l , weak/CMB lensing	✓	X	✓	✓
Correlation function	✓	X	✓	✓
Halo model	✓	✓	X	✓

structure can be generated using the information from a `ccl_parameters` object and a `ccl_configuration` object.

`ccl_parameters` objects contain information about the cosmological parameters of a given model, and are initialized using one of the following routines (the full syntax for each function can be found in the header file `ccl_core.h`):

- `ccl_parameters_create(double Omega_c, double Omega_b, double Omega_k, double N_eff, double *mnu, ccl_mnu_type_label mnu_type, double w0, double wa, double h, double norm_pk, double n_s, int nz_mgrowth, double *zarr_mgrowth, double *dfarr_mgrowth, int *status)`: general `ccl_parameters` constructor supporting all the models described above.
- `ccl_parameters_create_flat_lcdm(...)`: particular constructor for flat Λ CDM cosmologies.

The argument `norm_pk` can be used to specify the power spectrum normalization in terms of either σ_8 or A_s . The `ccl_parameters_create` functions assume σ_8 normalization if `norm_pk` > 1.0e - 5 and A_s normalization otherwise.

`ccl_configuration` objects contain information about the prescriptions to be used to compute transfer functions, power spectra, mass functions, etc. A default `ccl_configuration` object is made available as `default_config`, which specifies that CLASS will be used to compute transfer functions, HaloFit will be used to calculate the matter power spectrum, there will be no impact of baryons included and the Tinker 2010 prescription will be used to compute the halo mass function.

After initializing instances of `ccl_parameters` and `ccl_configuration`, use the function `ccl_cosmology_create(ccl_parameters, ccl_configuration)` to return a pointer to a `ccl_cosmology` structure. You will need to pass this pointer around to every CCL function.

An example of using CCL is provided in Section 6. The README file has additional extensive documentation for the example run, as well as installation.

Creating a cosmology with massive neutrinos—In the parameter construction routines above, `mnu` is a pointer to either a single value, to be interpreted as the sum of neutrino masses, or to an array containing the three neutrino masses, both in eV. `mnu_type` is a label which indicates whether `mnu` points to sum of the masses or to an array of three mass values. In the former case, `mnu_type` also defines which convention should be used to split the sum into three neutrino masses for calculations (options are normal hierarchy, inverted hierarchy, or an equal split).

To set up a cosmology with massive neutrinos, the user should pass `mnu`, `mnu_type`, and `N_eff` to the parameter construction routine. When working from the python wrapper, it suffices to pass `mnu` and `N_eff`; CCL will infer whether `mnu` is a set of masses or a sum. In the latter case, the default behaviour is to split the sum into masses consistent with the normal hierarchy, but an inverted hierarchy or equal splitting can be requested by passing `mnu_type`.

In the case where `mnu` corresponds to a sum, we first allocate the three neutrino masses according to the requested convention. The default convention is the normal hierarchy, but users may also request either an inverted hierarchy or a split of the sum into three equal masses. In the latter case it is trivial to compute the three masses. If splitting with respect to the normal or inverted hierarchy is desired, the mass calculation of the three masses is only marginally more complicated. The relevant known quantity which has been determined via particle physics experiments is the square of the difference of neutrino masses (up to a sign for one of the differences, hence the two possible hierarchies, see [Lesgourgues & Pastor 2012](#); [Lattanzi & Gerbino 2017](#)). Because we know the square of the differences rather than the differences themselves, we must solve a set of quadratic equations for the

neutrino masses. This is accomplished via a simple implementation of Newton's method, which converges to within machine precision in a few iterations.

Having then a set of three masses regardless of `mnue_type`, we check for which of the three masses the corresponding neutrino species is non-relativistic today ($m_\nu > 0.00017$, [Lesgourgues & Pastor 2012](#)), and obtain a number of massive neutrinos `N_nu_mass`. We use this along with the `N_eff` value to set the number of relativistic neutrinos species `N_nu_rel`. We must be slightly careful in doing so, as for massive neutrinos only we follow CLASS in modifying the relationship between the temperature of the CMB and the neutrino temperature:

$$T_\nu^{\text{eff}} = T_{\text{CMB}} T_{\text{NCDM}} \quad (1)$$

where the above defines T_{NCDM} , an adhoc modification to the equality between T_{CMB} and T_ν^{eff} . We follow the nomenclature of CLASS here, but we emphasize that T_{NCDM} is a dimensionless scaling factor, not a temperature. Setting $T_{\text{NCDM}} = 0.71611$ ensures that $m_\nu/\Omega_\nu^0 = 93.14\text{eV}$, in agreement with second-order theoretical calculations which correctly take into account QED effects and electron / positron annihilation ([Mangano et al. 2005](#)). Therefore to get `N_nu_rel` consistent with the `N_eff` passed by the user, we do:

$$\text{N_nu_rel} = \text{N_eff} - (T_{\text{NCDM}})^4 \left(\frac{4}{11} \right)^{-\frac{4}{3}} \text{N_nu_mass}. \quad (2)$$

For easier initiation of cosmologies with massive neutrinos, the suffix '`_nu`' may be appended to the last four `ccl_parameters_create` functions in the previous section. Using these functions without the `_nu` suffix will set the neutrino masses to 0 and the effective number of neutrino species to 3.046.

It may sometimes be preferable or necessarily to specify a cosmology in terms of Ω_ν^0 for massive neutrinos instead of m_ν . To facilitate this, CCL includes a convenience function `ccl_nu_masses`, which takes as input Ω_ν^0 for massive neutrinos, the temperature of the CMB, and a label specifying how the neutrino mass should be split amongst species similarly to above. It then outputs a pointer to the resulting neutrino mass(es).

4.4. Distances

The routines described in this subsection are implemented in `ccl_background.c`.

The Hubble parameter is calculated as

$$\frac{H(a)}{H_0} = a^{-3/2} \left(\Omega_{M,0} + \Omega_{\Lambda,0} a^{-3(w_0+w_a)} \exp[3w_a(a-1)] + \Omega_{K,0} a + (\Omega_{g,0} + \Omega_{\nu,\text{rel}}) a^{-1} + \Omega_{\nu,\text{m}}(a) a^3 \right)^{\frac{1}{2}}. \quad (3)$$

The radial comoving distance is calculated via a numerical integral,

$$\chi(a) = c \int_a^1 \frac{da'}{a'^2 H(a')}. \quad (4)$$

The transverse comoving distance is computed in terms of the radial comoving distance as:

$$r(\chi) = \begin{cases} k^{-1/2} \sin(k^{1/2} \chi) & k > 0 \\ \chi & k = 0 \\ |k|^{-1/2} \sinh(|k|^{1/2} \chi) & k < 0 \end{cases} \quad (5)$$

The usual angular diameter distance is $d_A = a r(a)$, and the luminosity distance is $d_L = r(a)/a$.

CCL can also compute the distance modulus, defined as,

$$\mu = 5 \log_{10}(d_L/\text{pc}) - 5 \quad (6)$$

and $a(\chi)$, the inverse of $\chi(a)$.

4.5. Density parameter functions

The routines described in this subsection are implemented in `ccl_background.c`.

The density parameter functions $\Omega_X(a)$ can be calculated for six components:

- matter density parameter $\Omega_M(a) = \Omega_{M,0} H_0^2 / (a^3 H^2(a))$,
- dark energy density parameter $\Omega_{\Lambda}(a) = \Omega_{\Lambda,0} a^{-3(1+w_0+w_a)} \exp[3w_a(a-1)] H_0^2 / H^2(a)$,
- radiation density parameter $\Omega_g(a) = \Omega_{g,0} H_0^2 / (a^4 H^2(a))$,
- curvature density parameter $\Omega_K(a) = \Omega_{K,0} H_0^2 / (a^2 H^2(a))$,

- massless neutrino density parameter $\Omega_{\nu,\text{rel}}(a) = \Omega_{\nu,\text{rel},0} H_0^2 / (a^4 H^2(a))$,
- massive neutrino density parameter $\Omega_{\nu,\text{m}}(a)$,

all using the Hubble parameter defined in equation 3.

For massive neutrinos, $\Omega_{\nu,\text{m}}(a)$ is calculated by calling a set of functions contained in `ccl_neutrinos.c`. For each species of massive neutrino with mass m_ν^i , we define

$$\tilde{m}^i = \frac{m_\nu^i a}{T_\nu^{\text{eff}}} \quad (7)$$

in units such that \tilde{m} is dimensionless. We conduct once the phase-space integral required to get the neutrino density (the integral over x in equation 8 below), and store the result as a `gsl` spline for subsequent access. Given then the value of this integral, we multiply by appropriate factors to obtain $\Omega_{\nu,\text{m}}(a)$:

$$\Omega_{\nu,\text{m}}(a) = \sum_{i=1}^{N_\nu} \frac{8\pi^2 (\pi k_b)^3 k_b}{15 (ch_P)^3} \frac{8\pi G}{3h^2 c^2} \left(\frac{T_\nu^{\text{eff}}}{a} \right)^4 \left(\frac{7}{8} \int_0^{x_{\text{max}}} dx x^2 \frac{\sqrt{x^2 + (\tilde{m}^i)^2}}{\exp(x) + 1} \right) \quad (8)$$

where h_P is Planck's constant and h is $H_0/100$ with H_0 in units of $\text{km} / \text{s} / \text{Mpc}$. x_{max} is set to 1000. The final bracketed term which includes the phase-space integral can be simplified in the limit where \tilde{m} is very large or very small: for small \tilde{m} , it is set to $\frac{7}{8}$, and for large \tilde{m} , it becomes $\frac{5\zeta(3)}{18\pi^4} \tilde{m} \sim 0.2776\mu$.

4.6. Functions of the physical density

The routines described in this subsection are implemented in `ccl_background.c`.

The physical density $\rho_X(a)$ can be calculated for seven components:

- critical density $\rho_{\text{crit}}(a) = \frac{3H^2(a)}{8\pi G} = \rho_{\text{crit},0} H^2(a) / H_0^2$,
- matter density $\rho_M(a) = \rho_{\text{crit}}(a) \Omega_M(a) = \rho_{\text{crit},0} \Omega_{M,0} / a^3$,
- dark energy density parameter $\rho_\Lambda(a) = \rho_{\text{crit},0} \Omega_{\Lambda,0} a^{-3(1+w_0+w_a)} \exp[3w_a(a-1)]$,
- radiation density parameter $\rho_g(a) = \rho_{\text{crit},0} \Omega_{g,0} / a^4$,
- curvature density parameter $\rho_K(a) = \rho_{\text{crit},0} \Omega_{K,0} / a^2$,
- massless neutrino density parameter $\rho_{\nu,\text{rel}}(a) = \rho_{\text{crit},0} \Omega_{\nu,\text{rel},0} / a^4$,

- massive neutrino density parameter $\Omega_{\nu,m}(a) = \rho_{\text{crit},0}\Omega_{\nu,m}(a)H^2(a)/H_0^2$,

where $\Omega_{\nu,m}(a)$ is given by equation 8 and the Hubble parameter by equation 3. CCL moreover allows for comoving physical densities $\rho_{X,\text{comoving}}(a) = \rho_X(a)a^3$.

4.7. Growth function

The routines described in this subsection are implemented in `ccl_background.c`. To compute the growth function, $D(a)$, the growth factor of matter perturbations, CCL solves the following differential equation:

$$\frac{d}{da} \left(a^3 H(a) \frac{dD}{da} \right) = \frac{3}{2} \Omega_M(a) a H(a) D, \quad (9)$$

using a Runge-Kutta Cash-Karp algorithm.

In doing this, CCL simultaneously computes the growth rate $f(a)$, defined as:

$$f(a) = \frac{d \ln D}{d \ln a}. \quad (10)$$

CCL provides different functions that return the growth normalized to $D(a = 1) = 1$ and to $D(a \ll 1) \rightarrow a$.

Note that the above is strictly valid for a Universe containing only dust-like matter components. A scale-independent growth rate is, for example, ill-defined in the presence of massive neutrinos; therefore CCL will raise an error if the user attempts to calculate the growth rate or growth factor in a cosmology with massive neutrinos.

Currently CCL allows for an alternative ‘modified gravity’ cosmological model defined by a regular background $(w_0 + w_a)\text{CDM}$ (with arbitrary K) as well as a user-defined $\Delta f(a)$, such that the true growth rate in this model is given by $f(a) = f_0(a) + \Delta f(a)$, where $f_0(a)$ is the growth rate in the background model. Note that this model is only consistently implemented with regards to the computation of the linear growth factor and growth rates (which will also scale the linear power spectrum). All other CCL functions (including the non-linear power spectrum) will ignore these modifications. This model, and the interpretation of the predictions given by CCL, should therefore be used with care.

4.8. Matter power spectrum

There are several options for obtaining the matter power spectrum in CCL. The routines described in this subsection are implemented in `ccl_power.c`.

4.8.1. BBKS

CCL implements the analytical BBKS approximation to the transfer function (Bardeen et al. 1986), given by

$$T(q \equiv k/\Gamma h \text{Mpc}^{-1}) = \frac{\ln[1 + 2.34q]}{2.34q} [1 + 3.89q + (16.2q)^2 + (5.47q)^3 + (6.71q)^4]^{-0.25} \quad (11)$$

where $\Gamma = \Omega_m h$. The power spectrum is related to the transfer function by $P(k) = 2\pi^2 \Delta^2(k)/k^3 \propto T^2(k)k^{n_s}$, where $\Delta(k)$ is the dimensionless power spectrum and n_s is the spectral index. The normalization of the power spectrum is defined at $z = 0$ by setting σ_8 to its value today. The BBKS power spectrum option is primarily used as a precisely-defined input for testing the numerical accuracy of CCL routines (as described in Sect. 5), and it is not recommended for other uses.

4.8.2. Eisenstein and Hu

CCL also provides an approximation to the matter power spectrum as implemented by Eisenstein & Hu (1998) (E&H; we refer the reader to this paper for a detailed discussion of the fitting formulae).¹⁵

The Eisenstein & Hu and BBKS approximations are not very accurate (generally only to within a few percent), and so should not be used to derive precise cosmological constraints. They are, however, computationally faster, and therefore useful for code testing and comparison.

4.8.3. CLASS

The fiducial configuration calls the CLASS software (Blas et al. 2011) within CCL to obtain either linear or nonlinear matter power spectra at given redshifts. On initializing the cosmology object, we construct a bi-dimensional spline in k and the scale-factor which is then evaluated by the relevant routines to obtain the matter power spectrum at the desired wavenumber and redshift. The relevant routines

¹⁵ Note that the implementation in CCL modifies Eq. 5 of Eisenstein & Hu (1998) using $a^{-1} = 1 + z$ instead of the approximation $a^{-1} \sim z$. The difference in the resulting power spectra is negligible, but larger than 1 part in 10^4 for $k < 10 h \text{Mpc}^{-1}$.

can be found within `ccl_power.c`. CLASS currently computes the non-linear power spectrum using the HaloFit prescription of [Takahashi et al. \(2012\)](#).

As discussed in Section 2.7, the user can compile CCL with an external version of CLASS as well.

4.8.4. Cosmic emulator

The cosmic emulator of [Lawrence et al. \(2017\)](#) is integrated into CCL and it is available as one of the matter power spectrum and transfer function methods (both have to be specified). The cosmic emulator provides predictions for the matter power spectrum based on an interpolation over simulation outputs spanning a defined set of cosmological parameter values.

The emulator provides accurate predictions for the nonlinear matter power spectrum, at the 1% level, for $z \leq 2$ and in the wavenumber range $k = [10^{-3}, 5] \text{ Mpc}^{-1}$. If a redshift above $z = 2$ is passed, the emulator will quit and return an error message. For k values below and above the previously specified range, we extrapolate in the manner specified in the following section.

The allowed range of cosmological parameters is as follows:

$$\begin{aligned}
 0.12 &\leq \Omega_m h^2 \leq 0.155, \\
 0.0215 &\leq \Omega_b h^2 \leq 0.0235, \\
 0.7 &\leq \sigma_8 \leq 0.9, \\
 0.55 &\leq h \leq 0.85, \\
 0.85 &\leq n_s \leq 1.05, \\
 -1.3 &\leq w_0 \leq -0.7, \\
 -1.73 &\leq w_a \leq -0.7, \\
 0.0 &\leq \Omega_\nu h^2 \leq 0.01.
 \end{aligned} \tag{12}$$

Actually, w_a and w_0 are constrained jointly to be $0.3 \leq (-w_0 - w_a)^{1/4}$. Note that CCL only allows a subregion within this parameter space. For models in which $w(z)$ crosses -1 at some given redshift, CLASS will crash because this value corresponds to a true cosmological constant, which by definition should have no perturbations.¹⁶ The linear matter power spectrum is still obtained from CLASS as described in the section above.

¹⁶ We thank Emilio Bellini and Miguel Zumalacárregui for clarifying this for us.

Neutrino species—The emulator is set up to consider $N_{\text{eff}} = 3.04$ and to allow the user to provide $\Omega_\nu h^2$ in order to set the neutrino mass, where it is assumed that the corresponding mass is split equally amongst three neutrinos. This is different from the standard CCL configuration, which takes as input the mass(es) of neutrinos in eV, m_ν . The assumption of an equal split of masses amongst three neutrino species is also different from the default CCL choice to split the mass amongst species according to the normal hierarchy. For best compatibility with the emulator, we therefore include a `ccl_configuration` element `emulator_neutrinos_method`, which defaults to `ccl_strict` but can be set to `ccl_equalize` if desired:

- `ccl_strict` requires the user to pass either a set of three equal neutrino masses, or to pass a sum of masses and to set `ccl_mnu_type` such that the sum is split equally amongst species. If other options are selected when the emulator is in use, CCL will raise an error and exit. This default option ensures full self-consistency within quantities calculated with a single CCL cosmology.
- `ccl_equalize` allows the user to pass an unequal set of neutrino masses, or to pass a sum with `ccl_mnu_type` set such that the sum is not split equally amongst species. In this case, CCL will pass redistributed equal neutrino masses to the emulator. This choice may result in internal inconsistency amongst different quantities calculated with the same CCL cosmology, or indeed even internal inconsistency between the linear and nonlinear parts of the same power spectrum. This option should only be selected for convenience if you are sure you don't care about the mass splitting between neutrino species.

Note also that because the emulator is constructed with $N_{\text{eff}} = 3.04$, the user is required to pass this when the emulator is in use. If this is not the case, CCL will quit and issue an error.

Notice that ideally we would like to pass a non-integer number of massive neutrino species for best compatibility with the emulator set-up. However, since this is not possible within CCL, we have opted to verify that neither the growth function nor the comoving radial distance computation are affected by this approximation to more than 10^{-4} in the range $0.01 < a < 1$, where a is the scale factor. We have verified this by comparing this prediction for a fiducial cosmology $\{\Omega_c = 0.27, \Omega_b = 0.049, h = 0.67, \sigma_8 = 0.8, n_s = 0.96\}$ with the following neutrino parameters: $\{N_{\nu, \text{rel}}, N_{\nu, \text{mass}}, m_\nu\} = \{0.00641, 3, 0.06\text{eV}\}$, $\{N_{\nu, \text{rel}}, N_{\nu, \text{mass}}, m_\nu\} = \{0, 3.04, 0.06\text{eV}\}$ and $\{N_{\nu, \text{rel}}, N_{\nu, \text{mass}}, m_\nu\} = \{0, 3.046, 0.06\text{eV}\}$. The discrepancy between distances and growth results between these choices of neutrino param-

eters can raise above 10^{-4} at $a < 0.01$ and the user should be mindful of this for their particular application.

4.8.5. Impact of baryons

CCL incorporates the impact of baryons on the total matter power spectrum via the “baryonic correction model” (BCM) of [Schneider & Teyssier \(2015\)](#). This is implemented through a flag in the configuration object, which currently accepts the following options: `ccl_nobaryons` or `ccl_bcm`. When `ccl_bcm` is set, the nonlinear matter power spectrum (whichever the method that provides it) is multiplied by a correction factor $F(k, z)$ which models the impact of baryons.

The main consequences of baryonic processes are: to suppress the power spectrum at intermediate scales ($k \sim$ a few h/Mpc) due to the ejection of gas by Active Galactic Nuclei feedback, and to enhance it at smaller scales due to enhanced cooling. Three effective parameters govern the contribution of baryonic processes to modifying the total matter power spectrum:

- $\log_{10}[M_c/(M_\odot/h)]$: the mass of the clusters responsible for feedback, which regulates the amount of suppression of the matter power spectrum at intermediate scales;
- η_b : a dimensionless parameter which determines the scale at which suppression peaks;
- and k_s [h/Mpc]: the wavenumber that determines the scale of the stellar profile.

If the BCM parameters are not specified and the user sets CCL to compute the power spectrum with baryonic feedback included, CCL will assume the default parameters of [Schneider & Teyssier \(2015\)](#). The user may pass these explicitly if desired.

Other baryonic impact models might be incorporated in the future as they become available.

4.8.6. Spline parameters & the INI file

All spline and grid parameters relevant for computing quantities such as distances, growth functions, power spectra, and halo mass functions are defined in the `ccl_params.ini` file in the `include` folder of the repository. This file allows the user to configure the following constants:

- `A_SPLINE_NLOG`: number of points in the logarithmic part of the scale factor spline. The default is `A_SPLINE_NLOG= 250`.
- `A_SPLINE_NA`: number of points in the linear part of the scale factor spline. The default is `A_SPLINE_NA= 250`.
- `A_SPLINE_MINLOG`: minimum value for the scale factor spline. The default is `A_SPLINE_MINLOG= 0.0001`. This only applies to background quantities.
- `A_SPLINE_MIN`: maximum value for the logarithmic part and minimum value for the linear part of the scale factor spline. The default is `A_SPLINE_MIN= 0.01`. This only applies to background quantities.
- `A_SPLINE_MAX`: maximum value for the scale factor spline. The default is `A_SPLINE_MAX= 1`.
- `LOGM_SPLINE_DELTA`: spacing of the mass function spline (logarithm). The default is `LOGM_SPLINE_DELTA= 0.025`.
- `LOGM_SPLINE_NM`: number of points in the mass function spline (logarithm). The default is `LOGM_SPLINE_NA= 440`.
- `LOGM_SPLINE_MIN`: minimum value for the mass function spline (logarithm). The default is `LOGM_SPLINE_MIN= 6`.
- `LOGM_SPLINE_MAX`: maximum value for the mass function spline (logarithm). The default is `LOGM_SPLINE_MAX= 17`.
- `A_SPLINE_NLOG_PK`: number of bins for the logarithmic part of the scale factor in the case of two-dimensional splines (where the second variable is the wavenumber). The default is `A_SPLINE_NLOG_PK= 11`.
- `A_SPLINE_NA_PK`: number of bins for the linear part of the scale factor in the case of two-dimensional splines (where the second variable is the wavenumber). The default is `A_SPLINE_NA_PK= 40`. In the case of the emulator's non-linear power spectrum, the maximum wavenumber is `K_MAX_SPLINE= 5/Mpc`, the interpolation is only linear and we use `A_SPLINE_NA_PK= 40` as default.
- `A_SPLINE_MINLOG_PK`: minimum value for the scale factor spline. The default is `A_SPLINE_MINLOG_PK= 0.01`. This only applies for the 2D power spectrum splines. For the cosmic emulator and in the case of the nonlinear matter

power spectrum, we use a linear spline only, adopting $A_SPLINE_MIN_PK=1/3$.

- $A_SPLINE_MIN_PK$: maximum value for the logarithmic part and minimum value for the linear part of the scale factor spline. The default is $A_SPLINE_MIN_PK=0.1$. This only applies for the 2D power spectrum splines.
- K_MAX_SPLINE : The maximum value of wavenumber considered in the spline. This is explained in more detail in the coming subsections. The default is $K_MAX_SPLINE=50/\text{Mpc}$. In the case of the emulator's nonlinear power spectrum, the maximum wavenumber is $K_MAX_SPLINE=5/\text{Mpc}$.
- K_MAX : The maximum value of wavenumber when integrating over k . The default is $K_MAX=1000/\text{Mpc}$.
- K_MIN : The minimum value of wavenumber when integrating over k . The default is $K_MIN=5 \times 10^{-5}/\text{Mpc}$.
- N_K : Number of bins per decade for the wavenumber. The default is $N_K=167$.
- N_K_3DCOR : Number of bins per decade for the wavenumber in the 3d correlation function calculation. The default is $N_K_3DCOR=100,000$.

The precision parameters of GSL routines can also be set in `ccl_params.ini`. The parameters are organized in a hierarchal fashion, such that more specialized parameters take precedence over more general ones. For example, there is a general tolerance parameter, a tolerance parameter for integrals, and a tolerance parameter for the Limber integral. By default all are set to the value of the general tolerance. Changing the integration tolerance changes the tolerance for all integrals but not for root-finding routines, for example, and changing the Limber integral tolerance only affects that integral and no other. The parameters are:

- GSL_EPSREL : Relative tolerance for GSL routines. Default is 10^{-4} .
- $GSL_N_ITERATION$: Maximum number of iterations allowed for GSL routines. This parameter also controls the size of the integration workspaces. Default is 1000.
- $GSL_INTEGRATION_GAUSS_KRONROD_POINTS$: Number of Gauss-Kronrod points in the QAG integration routines. Default is $GSL_INTEG_GAUSS41$ (numerical value 4).
- $GSL_INTEGRATION_EPSREL$: Relative tolerance for GSL integration routines. Default is GSL_EPSREL .

- `GSL_INTEGRATION_DISTANCE_EPSREL`: Relative tolerance for GSL integration routines for distance calculations. Default is 10^{-6} .
- `GSL_INTEGRATION_DNDZ_EPSREL`: Relative tolerance for GSL integration routines for $\frac{dN}{dz}$ calculations. Default is 10^{-6} .
- `GSL_INTEGRATION_SIGMAR_EPSREL`: Relative tolerance for GSL integration routines for σ_R calculations. Default is 10^{-5} .
- `GSL_INTEGRATION_NU_EPSREL`: Relative tolerance for GSL integration routines for neutrino calculations. Default is 10^{-7} .
- `GSL_INTEGRATION_NU_EPSABS`: Absolute tolerance for GSL integration routines for neutrino calculations. Default is 10^{-7} .
- `GSL_INTEGRATION_LIMBER_GAUSS_KRONROD_POINTS`: Number of Gauss-Kronrod points in the QAG integration routines for the Limber integral. Default is `GSL_INTEGRATION_GAUSS_KRONROD_POINTS`.
- `GSL_INTEGRATION_LIMBER_EPSREL`: Relative tolerance for GSL integration routines for Limber integral. Default is `GSL_EPSREL`.
- `GSL_ROOT_EPSREL`: Relative tolerance for GSL root-finding routines. Default is `GSL_EPSREL`.
- `GSL_ROOT_N_ITERATION`: Maximum number of iterations allowed for GSL root-finding routines. Default is `GSL_N_ITERATION`.
- `GSL_ODE_GROWTH_EPSREL`: Relative tolerance for GSL ODE-solving routines for growth factor calculation. Default is 10^{-6} .

The GSL parameters are initialized to their default values and do not need to be listed in `ccl_params.ini` if no adjustments are necessary.

Note that a copy of `ccl_params.ini` is installed along with the library, so changing the version of this file inside the source directory will not have any effect unless you reinstall.

For the matter power spectrum, the spline is performed in two variables: the logarithmically-spaced wavenumber and the linearly-spaced scale factor. Splineing the CLASS output leads to some precision loss (compared to direct outputs from CLASS). We quantify this, along with the impact of extrapolation, in the following subsection.

4.8.7. Extrapolation for the nonlinear power spectrum

The computation of the power spectrum from CLASS can be significantly sped up by extrapolating in the range $k > K_MAX_SPLINE$ and $k < K_MIN_SPLINE$. In this section, we describe the implementation of the extrapolation and the accuracy attained. These tests are performed in a flat Λ CDM cosmology with $\Omega_c = 0.25$, $\Omega_b = 0.05$, $A_s = 2.1 \times 10^{-9}$, $h = 0.7$ and $n_s = 0.96$.

We first describe the extrapolation at high wavenumbers. The introduction of the parameter `K_MAX_SPLINE` allows us to spline the matter power spectrum within the `cosmo` structure up to that value of k (in units of $1/\text{Mpc}$). A separate `K_MAX` parameter sets the limit for evaluation of the matter power spectrum. The range between $K_MAX_SPLINE < k < K_MAX$ is evaluated by performing a second order Taylor expansion in $\ln k$ within the static routine `ccl_power_extrapol_highk`.

First, we compute the first and second derivative of the $\ln P(k, z)$ at $k_0 = K_MAX_SPLINE - 2\Delta \ln k$ by computing the numerical derivatives by finite differences using GSL. The fiducial choice for $\Delta \ln k$ is 10^{-2} . We then apply a second order Taylor expansion to extrapolate the matter power spectrum to $k > K_MAX_SPLINE$. The Taylor expansion gives

$$\ln P(k, z) \simeq \ln P(k_0, z) + \frac{d \ln P}{d \ln k}(\ln k_0, z)(\ln k - \ln k_0) + \frac{1}{2} \frac{d^2 \ln P}{d \ln k^2}(\ln k_0, z)(\ln k - \ln k_0)^2. \quad (13)$$

The accuracy of this approximation is shown in Figure 1 for redshifts $z = 0$, $z = 3$ and $z = 20$. We compare the nonlinear matter power spectrum at these redshifts computed with the previously described approximation, to the matter power spectrum obtained by setting the power spectrum splines to high values. We find that for typical values of $\Delta \ln k = 10^{-2}$ and $K_MAX_SPLINE = 50/\text{Mpc}$, $\ln P$ has converged to an accuracy that surpasses the expected impact of baryonic effects on the matter power spectrum at $k > 10/\text{Mpc}$. (For an estimate of the impact of baryons on the total matter power spectrum, see [Schneider & Teyssier 2015](#).) The lower `K_MAX_SPLINE` is, the faster CCL will run. The optimum choice of `K_MAX_SPLINE` is left to the user for their particular application.

We also extrapolate the power spectrum at small wavenumbers within the static routine `ccl_power_extrapol_lowk`. In this case, the power spectrum below `K_MIN_SPLINE` is obtained by a power-law extrapolation with index n_s :

$$\log P(k < K_MIN_SPLINE, z) = \log P(K_MIN_SPLINE, z) + n_s(\log k - \log K_MIN_SPLINE) \quad (14)$$

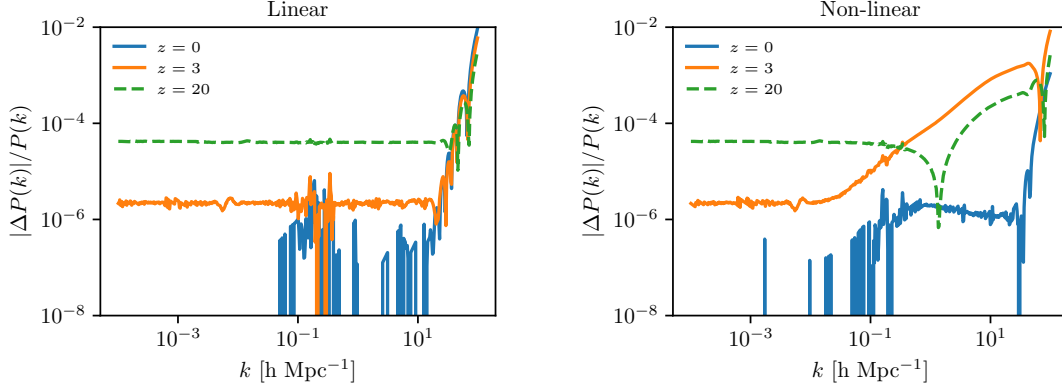


Figure 1. The relative error compared to power spectra produced with high values of the power spectrum splines, P_{fid} , produced by splining the matter power spectrum up to $K_MAX_SPLINE = 50 \text{ Mpc}^{-1}$ and extrapolating beyond this value with a second order Taylor expansion the natural logarithm of the matter power spectrum. The left panel shows the relative errors for the linear matter power spectrum at $z = 0$, $z = 3$ and $z = 20$. The right panel shows the results for the non-linear matter power spectrum at the same redshifts. The standard CCL parameters adopted are those corresponding to the black dashed curve. For comparison, the impact of baryonic physics on the matter power spectrum is $\sim 10\%$ at $k = 1 \text{ Mpc}^{-1}$ (Schneider & Teyssier 2015).

The value adopted for K_MIN_SPLINE depends on the choice of power spectrum method and is not currently accessible to the user via the .ini file. For CLASS and the nonlinear power spectrum, we adopt K_MIN_SPLINE that coincides with the smallest wavenumber output by CLASS, $K_MIN_SPLINE = 7 \times 10^{-6} / \text{Mpc}$. Note that this parameter is different from K_MIN , which sets the minimum k for integrations and which is set by default to $K_MIN = 5 \times 10^{-5} / \text{Mpc}$. Hence, in practice, no extrapolation is occurring in this case, unless the user specifically asks for an output power spectra below K_MIN for their own purposes.

For BBKS, the power spectrum is computed analytically at all k , there is no extrapolation. For the Eisenstein & Hu implementation, the splines of the power spectrum span $K_MIN < k < K_MAX_SPLINE$, so there is only extrapolation at high k . For the non-linear matter power spectrum from the emulator, K_MIN_SPLINE and K_MAX_SPLINE are set to fixed values that are determined from the range of validity of the emulator: $K_MIN_SPLINE = 10^{-3} \text{ Mpc}^{-1}$ and $K_MAX_SPLINE = 5 \text{ Mpc}^{-1}$.

4.8.8. Extrapolation for the linear power spectrum

With the implementation described in the previous section, the power spectrum splines are initialized up to K_MAX_SPLINE . This is also true for the linear matter power spectrum, which is used within CCL in particular to obtain σ_8 (see Eq. 47). We have tested here how the procedure described in the previous section affects

the convergence of the linear matter power spectrum. The result is shown in Figure 1. For some applications that use the linear power spectrum, the user might need to increase the value of `K_MAX_SPLINE`.

As in the previous section, the power spectrum at small wavenumber is extrapolated using a power-law. This extrapolation is performed below a fiducial value of `K_MIN_SPLINE` that coincides with the smallest wavenumber output by `CLASS`, as in the case of the nonlinear power spectrum described above.

We have found that changing `N_A` to 200, or changing the sampling of the wavenumber to 5000 points, does not change the results presented in Figures 1 in this section.

4.8.9. Wishlist for the future

We plan to implement the following power spectrum methods in the future:

- CAMB,
- other emulators,
- HOD.

4.8.10. Normalization of the power spectrum

There are two alternative schemes for normalization of the matter power spectrum. The first one is to specify the value of A_s , the amplitude of the primordial power spectrum, which is passed directly to `CLASS`. This option is available in the case of the linear/nonlinear matter power spectrum implementation. For these, as well as for BBKS and E&H transfer functions, there is the additional option to set the normalization of the matter power spectrum by specifying σ_8 , the RMS density contrast averaged over spheres of radius $8h^{-1}\text{Mpc}$. The computation of σ_8 is described in Section 4.11.

In practice, there is only one argument that encodes the normalization. This is the argument `norm_pk`, which can be passed the power spectrum normalization parameterized by σ_8 or A_s . As noted above, `ccl_parameters_create` switches to σ_8 normalization if `norm_pk > 10-5`, and to A_s normalization otherwise.

In the `python` implementation, CCL allows for either `σ8` or `As` to be passed as parameters.

4.9. Angular power spectra

In this section we will distinguish between *observables* (quantities observed on the sky, such as number counts in a redshift bin, shear or CMB temperature fluctuations) and *contributions* to the total observed fluctuations of these observables (such as the biased matter density term in number counts, redshift-space distortions, magnification, ISW, etc.). The routines described in this subsection are implemented in `ccl_cls.cc`.

4.9.1. Exact expressions

The angular power spectrum between two observables a and b can be written as:

$$C_\ell^{ab} = 4\pi \int_0^\infty \frac{dk}{k} \mathcal{P}_\Phi(k) \Delta_\ell^a(k) \Delta_\ell^b(k), \quad (15)$$

where $\mathcal{P}_\Phi(k)$ is the dimensionless power spectrum of the primordial curvature perturbations, and Δ^a and Δ^b are, using the terminology of CLASS, the transfer functions corresponding to these observables. Each transfer function will receive contributions from different terms. Currently CCL supports two observables (also labelled “tracers”), number counts and galaxy shape distortions, with the following contributions:

Number counts.—The transfer function for number counts can be decomposed into three terms: $\Delta^{\text{NC}} = \Delta^{\text{D}} + \Delta^{\text{RSD}} + \Delta^{\text{M}}$, where

- Δ^{D} is the standard density term proportional to the matter density:

$$\Delta_\ell^{\text{D}}(k) = \int dz p_z(z) b(z) T_\delta(k, z) j_\ell(k\chi(z)), \quad (16)$$

where T_δ is the matter transfer function. Note that CCL currently does not support non-linear or scale-dependent bias. Here, $p_z(z)$ is the normalized distribution of sources in redshift (selection function). Thus CCL understands each individual redshift bin as a separate “observable”.

- Δ^{RSD} is the linear contribution from redshift-space distortions:

$$\Delta_\ell^{\text{RSD}}(k) = \int dz p_z(z) \frac{(1+z)p_z(z)}{H(z)} T_\theta(k, z) j_\ell''(k\chi(z)), \quad (17)$$

where $T_\theta(k, z)$ is the transfer function of θ , the divergence of the comoving velocity field. $T_\theta(k, z)$ depends on the growth, which CCL does not compute for massive neutrino cosmologies; therefore at this time an attempt to create a number count tracer in a cosmology with massive neutrinos will cause CCL to raise an error. C_ℓ is instead computed assuming a linear-theory relation between the matter overdensity and peculiar velocity fields. While this should not be problematic for wide photometric redshift bins, users should exercise care when interpreting results for narrow window functions.

- Δ^M is the contribution from magnification lensing:

$$\Delta_\ell^M(k) = -\ell(\ell + 1) \int \frac{dz}{H(z)} W^M(z) T_{\phi+\psi}(k, z) j_\ell(k\chi(z)), \quad (18)$$

where $T_{\phi+\psi}$ is the transfer function for the Newtonian-gauge scalar metric perturbations, and W^M is the magnification window function:

$$W^M(z) \equiv \int_z^\infty dz' p_z(z') \frac{2 - 5s(z')}{2} \frac{r(\chi(z') - \chi(z))}{r(\chi(z'))}. \quad (19)$$

Here $s(z)$ is the magnification bias, given as the logarithmic derivative of the number of sources with magnitude limit, and $r(\chi)$ is the angular comoving distance (see Eq. 5).

Note that CCL currently does not compute relativistic corrections to number counts [Challinor & Lewis \(2011\)](#); [Bonvin & Durrer \(2011\)](#). Although these should be included in the future, their contribution to the total fluctuation is largely subdominant (see [Alonso et al. \(2015\)](#) and the two references above), and therefore it is safe to work without them in most cases.

Galaxy shape distortions.—The transfer function for shape distortions is currently decomposed into two terms: $\Delta^{\text{SH}} = \Delta^{\text{WL}} + \Delta^{\text{IA}}$, where

- Δ^L is the standard lensing contribution:

$$\Delta_\ell^L(k) = -\frac{1}{2} \sqrt{\frac{(\ell + 2)!}{(\ell - 2)!}} \int \frac{dz}{H(z)} W^L(z) T_{\phi+\psi}(k, z) j_\ell(k\chi(z)), \quad (20)$$

where W^L is the lensing kernel, given by

$$W^L(z) \equiv \int_z^\infty dz' p_z(z') \frac{r(\chi(z') - \chi(z))}{r(\chi(z'))}. \quad (21)$$

- Δ^{IA} is the transfer function for intrinsic galaxy alignments. CCL currently supports the so-called “non-linear alignment model”, according to which the

galaxy inertia tensor is proportional the local tidal tensor [Hirata & Seljak \(2004\)](#); [Hirata et al. \(2007\)](#).

$$\Delta_{\ell}^{\text{IA}}(k) = \sqrt{\frac{(\ell+2)!}{(\ell-2)!}} \int dz p_z(z) b_{\text{IA}}(z) f_{\text{red}}(z) T_{\delta}(k, z) \frac{j_{\ell}(k\chi(z))}{(k\chi(z))^2}. \quad (22)$$

It is worth noting that the equations above should be modified for non-flat cosmologies by replacing the spherical Bessel functions j_{ℓ} with their hyperspherical counterparts [Kamionkowski & Spergel \(1994\)](#). Since the library currently only uses the Limber approximation (documented below), this is not currently an issue. It will be revisited in future versions of CCL.

CMB lensing.—The transfer function lensing convergence from a source at redshift z_S is given by:

$$\Delta_{\ell}^{\text{C}}(k) = -\frac{\ell(\ell+1)}{2} \int_0^{\chi_S} d\chi \frac{r(\chi_S) - r(\chi)}{r(\chi)r(\chi_S)} T_{\phi+\psi}(k, \chi) j_{\ell}(k\chi), \quad (23)$$

where $\chi_S \equiv \chi(z_S)$.

4.9.2. The Limber approximation

As shown above, computing each transfer function involves a radial projection (i.e. an integral over redshift or χ), and thus computing full power spectrum consists of a triple integral for each ℓ . This can be computationally intensive, but can be significantly simplified in certain regimes by using the Limber approximation, given by:

$$j_{\ell}(x) \simeq \sqrt{\frac{\pi}{2\ell+1}} \delta\left(\ell + \frac{1}{2} - x\right). \quad (24)$$

Thus for each k and ℓ we can define a radial distance $\chi_{\ell} \equiv (\ell + 1/2)/k$, with corresponding redshift z_{ℓ} . This approximation works best for wide radial kernels and high multipoles.

Substituting this in the expressions above, the simplified versions become:

$$C_{\ell}^{ab} = \frac{2}{2\ell+1} \int_0^{\infty} dk P_{\delta}(k, z_{\ell}) \tilde{\Delta}_{\ell}^a(k) \tilde{\Delta}_{\ell}^b(k). \quad (25)$$

where

$$\tilde{\Delta}_\ell^{\text{D}}(k) = p_z(z_\ell) b(z_\ell) H(z_\ell) \quad (26)$$

$$\tilde{\Delta}_\ell^{\text{RSD}}(k) = \frac{1+8\ell}{(2\ell+1)^2} p_z(z_\ell) f(z_\ell) H(z_\ell) - \quad (27)$$

$$\frac{4}{2\ell+3} \sqrt{\frac{2\ell+1}{2\ell+3}} p_z(z_{\ell+1}) f(z_{\ell+1}) H(z_{\ell+1}) \quad (28)$$

$$\tilde{\Delta}_\ell^{\text{M}}(k) = 3\Omega_{M,0}H_0^2 \frac{\ell(\ell+1)}{k^2} \frac{(1+z_\ell)}{r(\chi_\ell)} W^{\text{M}}(z_\ell) \quad (29)$$

$$\tilde{\Delta}_\ell^{\text{L}}(k) = \frac{3}{2}\Omega_{M,0}H_0^2 \sqrt{\frac{(\ell+2)!}{(\ell-2)!}} \frac{1}{k^2} \frac{1+z_\ell}{r(\chi_\ell)} W^{\text{L}}(z_\ell) \quad (30)$$

$$\tilde{\Delta}_\ell^{\text{IA}}(k) = \sqrt{\frac{(\ell+2)!}{(\ell-2)!}} \frac{p_z(z_\ell) b_{\text{IA}}(z_\ell) f_{\text{red}}(z_\ell) H(z_\ell)}{(\ell+1/2)^2} \quad (31)$$

$$\tilde{\Delta}_\ell^{\text{C}}(k) = \frac{3}{2}\Omega_{M,0}H_0^2 \ell(\ell+1) \frac{1+z_\ell}{k^2} \frac{r(\chi_{\text{S}}) - r(\chi_\ell)}{r(\chi_\ell)r(\chi_{\text{S}})} \Theta(\chi_\ell; 0, \chi_{\text{S}}). \quad (32)$$

Here $(\Theta(x; x_i, x_f))$ is a top-hat function (1 for $x \in [x_i, x_f]$ and 0 otherwise).

4.9.3. Beyond limber

Native CCL computation.

Note: This capability has been deprecated in v1 in favor of `Angpow`, described below. But it is still available in previous versions of the library.

CCL incorporates routines to compute the C_ℓ^{ab} angular power spectra as described above but without the Limber approximation. The algorithm performs first the integrals over z for both tracers, and ends with the k integral. This computation is much slower than using the Limber approximation, but it ends up with precise angular power spectra at low ℓ , and correct cross-correlations between tracers (the Limber approximation fails at reproducing the interference terms $j_\ell(x) \times j_\ell(x')$).

Some parameters are needed to define this integral. First, to fasten the computation the C_ℓ^{ab} function is computed for a selection of ℓ values (linearly spaced at low- ℓ and logarithmically spaced at high- ℓ) and then the function is splined. Then the integration step of the redshift integrals must be specified in terms of a comoving distance. It is recommended to start with a low value (< 3 Mpc) for a high precision integration, and then to release this parameter to achieve the user needs in terms of precision and rapidity. A logarithmic step in k must also be provided: it does not correspond to the integration step but to a computation step before splining the

transfer functions $\Delta_\ell^a(k)$. Last parameter, a minimum redshift can be given for the redshift integral bound so that the transfer functions are not computed near $z \approx 0$ where they can be numerically undefined.

The integration bounds in redshift are estimated automatically given the a redshift window so that the integration is preformed where the redshift window is relevant within a given precision (set by the `CCL_FRAC_RELEVANT` parameter). The integration bounds for the k integrals are defined automatically given the ℓ multipole and the comoving distances at play.

It is worth noting that the user can define a threshold multipole ℓ from which the C_ℓ^{ab} computation switches to the Limber approximation which is faster and generally relevant at high ℓ values.

Angpow.

The aim of the `Angpow` software (Campagne et al. 2017) is to compute the angular power spectra C_ℓ^{ab} without any Limber numerical approximation. `CCL` has been linked to the `Angpow` code, which is briefly described here.

The angular power spectrum for two shells C_ℓ^{ab} is computed in `Angpow` according to the following expression

$$C_\ell^{ab} = \iint_0^\infty dz dz' p_{z_1}(z_1) p_{z_2}(z') \times \int_0^\infty dk f_\ell(z, k) f_\ell(z', k). \quad (33)$$

The auxiliary function $f_\ell(z, k)$ can be defined without loss of generality as

$$f_\ell(z, k) \equiv \sqrt{\frac{2}{\pi}} k \sqrt{P(k, z)} \tilde{\Delta}_\ell(z, k) \quad (34)$$

with

- $P(k, z)$: the matter power spectrum at redshift z
- $\tilde{\Delta}_\ell(z, k)$: a function describing the physical processes such as matter density fluctuations, redshift-space distortions as described for instance in references Durrer (2008); Yoo et al. (2009); Yoo (2010); Challinor & Lewis (2011); Bonvin & Durrer (2011). Currently, the `Angpow` version delivered with `CCL` only can deal with galaxy clustering tracers (no lensing) and this without the magnification lensing term (equation 18). The incorporation of those transfer functions is left for future work, but in principle `Angpow` has already the capability to treat them. For now, for galaxy clustering tracers we defined $\tilde{\Delta}_\ell(z, k)$ as

$$\tilde{\Delta}_\ell(z, k) \approx b_{j_\ell}(k\chi(z)) - f(z) j_\ell''(k\chi(z)) \quad (35)$$

with $j_\ell(x)$ and $j_\ell''(x)$ the spherical Bessel function of order ℓ and its second derivative, and $f(a)$ the growth rate as defined subsection 4.7 (derivative of the growth function with respect to the scale factor a).

To proceed to a numerical evaluation of equation 33, Angpow first conducts inside the rectangle $[z_{1\min}, z_{1\max}] \times [z_{2\min}, z_{2\max}]$ given by the $p_z(z)$ selection functions a Cartesian product of one-dimensional (1D) quadrature defined by the set of sample nodes z_i and weights w_i . In practice, the Clenshaw-Curtis quadrature is used. The corresponding sampling points (z_{1i}, z_{2j}) are weighted by the product $w_i w_j$ using the 1D quadrature sample points and weights on both redshift regions with $i = 0, \dots, N_{z_1} - 1$ and $j = 0, \dots, N_{z_2} - 1$. Then, one gets the following approximation:

$$C_\ell^{ab} \approx \sum_{i=0}^{N_{z_1}-1} \sum_{j=0}^{N_{z_2}-1} w_i w_j p_{z_1}(z_i) p_{z_2}(z_j) \hat{P}_\ell(\chi_i, \chi_j) \quad (36)$$

with the notations $z_i = z_{1i}$, $z_j = z_{2j}$ and $\chi_i = \chi(z_{1i})$, $\chi_j = \chi(z_{2j})$ and

$$\hat{P}_\ell(z_i, z_j) = \int_0^\infty dk f_\ell(z_i, k) f_\ell(z_j, k), \quad (37)$$

To conduct the computation of such integral of highly oscillating functions we use the 3C-algorithm described in details in reference (Campagne et al. 2017). In brief this algorithm proceeds the following way:

1. the total integration k interval (eg. $[k_{\min}, k_{\max}]$) in equation (37) is cut on several k -sub-intervals;
2. on each sub-interval the functions $f_{i\ell}(k) = f_\ell(z_i, k)$ and $f_{j\ell}(k) = f_\ell(z_j, k)$ are projected onto Chebyshev series of order 2^N ;
3. the product of the two Chebyshev series is performed with a 2^{2N} Chebyshev series;
4. then, the integral on the sub-interval is computed thanks to the Clenshaw-Curtis quadrature.

All the Chebyshev expansions and the Clenshaw-Curtis quadrature are performed via the DCT-I fast transform of FFTW.

Thanks to the 3C-algorithm, the Angpow is able to compute the C_ℓ^{ab} in a fast and accurate way. It was tested against CLASS and the native CCL computation and can performed the computation an order of magnitude faster, which is more suitable for an extensive exploration of the cosmological parameter space ($\mathcal{O}(1s)$). Note that

Angpow is written in C++ with OpenMP, to distribute the computation of a single C_ℓ on a single thread. The computation can also be switch by the user to the faster Limber approximation setting a threshold multipole ℓ .

Precision tests.

The code has been compared with CLASS and the native CCL computation and all three softwares agrees perfectly if precision parameters are pushed to high levels.

A few parameters must be provided to set the precision of this computation. First the order of the Chebyshev polynomials is set to 2^{10} by default, and the number of k sub-intervals to 200, and we checked this is enough for the current uses. Then the redshift quadrature stepping is set automatically given the redshift windows to recover the native CCL computation boosted with high precision parameters: its precision is optimised so that the relative numerical error compared with the native method is two orders of magnitude below the relative cosmic variance $\sqrt{2/(2\ell+1)}$, from $\ell = 2$ to $\ell = 1000$. The k_{\min} and k_{\max} bounds are also automatically set given the current multipole ℓ and the comoving distance χ involved in the inner integral.

4.10. Correlation functions

The following expressions relating the angular power spectra and correlation functions are valid in the flat-sky approximation¹⁷. In all cases, $f_K(\chi)$ is comoving angular diameter distance, which differs from the radial comoving distance χ only in the case of cosmologies with non-zero curvature. The routines described in this subsection are implemented in `ccl_correlation.c`.

Galaxy-galaxy. The angular correlation function between two number-count tracers (labeled a and b here) is given by

$$\xi^{ab}(\theta) = \int d\ell \frac{\ell}{2\pi} C_\ell^{ab} J_0(\ell\theta), \quad (38)$$

where C_{ab} is the angular power spectrum between both tracers.

¹⁷ See the weak lensing review by [Bartelmann & Schneider \(2001\)](#), page 44 and [Joachimi & Bridle \(2010\)](#).

Lensing-lensing. The lensing correlation functions are ¹⁸

$$\xi_+^{ab}(\theta) = \int_0^\infty d\ell \frac{\ell}{2\pi} J_0(\ell\theta) C_\ell^{ab}, \quad (39)$$

$$\xi_-^{ab}(\theta) = \int_0^\infty d\ell \frac{\ell}{2\pi} J_4(\ell\theta) C_\ell^{ab}, \quad (40)$$

where the angular lensing convergence power spectrum C_ℓ^{ab} is given above (see Equations 20 and 25).

Galaxy-lensing. The correlation between a number count tracer a and a shear tracer b is given by

$$\xi^{ab}(\theta) = \int d\ell \frac{\ell}{2\pi} C_\ell^{ab} J_2(\ell\theta), \quad (41)$$

Note that, in the above, “Galaxy” and “Lensing” can be replaced by any spin-0 and spin-2 fields on the sphere respectively (e.g. the CMB lensing convergence would play the same role as the galaxy overdensity field in all the formulas above).

3d spatial correlation function. In addition to the angular correlation functions, the 3-dimensional spatial correlation function $\xi(r)$ is also calculated from the power spectrum $P(k)$ using

$$\xi(r) = \frac{1}{2\pi^2} \int dk k^2 P(k) \frac{\sin(kr)}{kr} \quad (42)$$

To evaluate the numerical integral in the correlation functions, we make use of the public code FFTlog¹⁹(Hamilton 2000; Talman 2009). In brief, FFTlog works on functions periodic in log space, by writing the Hankel Transform as a convolution between Bessel functions and the function of interest (in this case either C_ℓ or $P(k)$). A version of this code is included in CCL with minor modifications.

4.11. Halo mass & halo bias functions

The routines described in this subsection are implemented in `ccl_massfunc.c`.

The halo mass function is implemented using several different definitions from the literature: Tinker et al. (2008), Tinker et al. (2010), Angulo et al. (2012), and Watson et al. (2013). All four models are tuned to simulation data and tested against

¹⁸ from Schneider 2002 and Bartelmann & Schneider section 6.4.1

¹⁹ <http://casa.colorado.edu/~ajsh/FFTLog/>

observational results. In addition, each of these fits has been implemented using the common halo definition of $\Delta = 200$, where a halo is defined with:

$$\bar{\rho}(r_\Delta) = \Delta \times \rho_m, \quad (43)$$

where a halo with size r_Δ has an average density $\bar{\rho}$ equal to the overdensity parameter Δ times the mean background density of the universe, ρ_m . Note that another common definition utilizes the critical density of the universe, ρ_c ; currently CCL requires that an external conversion by the end user between values of Δ with respect to the critical density to values of Δ as defined with respect to the mean density. In the future we plan to allow for self-consistent handling of critical density based definitions, though it is not implemented as of this build.

In addition to the usage of the most common definition, we have implemented an extension for two of the models. The Tinker 2010 model allows for a value of Δ to be given between the values of 200 and 3200 and interpolates the fitting parameters within this range in a space of $\log \Delta$ using splines. We also have implemented interpolation in the same range of Tinker 2008 Δ values. For both Tinker 2008 and Tinker 2010 models we have utilized spline interpolation through GSL routines in order to guarantee a match to specified fitting parameters at exact values of Δ . This fitting has slight deviation from the fit as expressed in Tinker 2010.

The halo mass function models implemented in CCL are tuned to simulations without massive neutrinos, therefore are not valid in cosmologies with massive neutrinos. Attempts to calculate the halo mass function, halo bias, or other related quantities within cosmologies with massive neutrinos will cause CCL to raise an error and quit.

With the exception of the Tinker 2010 model, we attempt to keep a common form to the multiplicity function whenever possible for ease of extension:

$$f(\sigma) = A \left[\left(\frac{\sigma}{b} \right)^{-a} + 1 \right] e^{-c/\sigma^2}, \quad (44)$$

where A , a , b , and c are fitting parameters that have additional redshift scaling and σ is the RMS variance of the density field smoothed on some scale M at some scale factor a . This basic form is modified for the [Angulo et al. \(2012\)](#) formulation. The resulting form is

$$f(\sigma) = A \left[\left(\frac{b}{\sigma} + 1 \right)^{-a} \right] e^{-c/\sigma^2}, \quad (45)$$

where the only change is in the formulation of the second term. Note that the fitting parameters in the [Angulo et al. \(2012\)](#) formulation do not contain any redshift dependence and the use of it is primarily for testing and benchmark purposes.

Each call to the halo mass function requires an assumed model (defined within the `ccl_configuration` structure contained in `ccl_cosmology`), in addition to a value of the halo mass and scale factor for which to evaluate the halo mass function. The currently implemented models can be called with the tags `config.mass_function_method = ccl_tinker, ccl_tinker10, ccl_angulo, or ccl_watson`. It returns the number density of halos in logarithmic mass bins, in the form $dn/d\log_{10} M$, where n is the number density of halos of a given mass and M is the input halo mass.

The halo mass M is related to σ by first computing the radius R that would enclose a mass M in a homogeneous Universe at $z = 0$:

$$M = \frac{H_0^2}{2G} R^3 \rightarrow \frac{M}{M_\odot} = 1.162 \times 10^{12} \Omega_M h^2 \left(\frac{R}{1 \text{ Mpc}} \right)^3. \quad (46)$$

The rms density contrast in spheres of radius R can then be computed as

$$\sigma_R^2 = \frac{1}{2\pi^2} \int dk k^2 P_k \tilde{W}_R^2(k) \quad (47)$$

where P_k is the matter power spectrum and $\tilde{W}(kR)$ is the Fourier transform of a spherical top hat window function,

$$\tilde{W}_R(k) = \frac{3}{(kR)^3} [\sin(kR) - kR \cos(kR)] \quad (48)$$

This function is directly implemented in CCL as well as a specific σ_8 function.

The [Tinker et al. \(2010\)](#) model parameterizes both the halo mass function and the halo bias in terms of the peak height, $\nu = \delta_c/\sigma(M)$, where δ_c is the critical density for collapse and is chosen to be 1.686 for this particular parameterization. We can then parameterize the halo function and halo bias as

$$b(\nu) = 1 - A \frac{\nu^a}{\nu^a + \delta_c^a} + B\nu^b + C\nu^c, f(\nu) = \alpha[1 + (\beta\nu)^{-2\phi}] \nu^{2\eta} e(-\gamma\nu^2/2). \quad (49)$$

The currently implemented model in CCL allows for an arbitrary overdensity Δ to be chosen, using the fitting functions provided in [Tinker et al. \(2010\)](#). Other halo model definitions are not included in the halo bias calculation, though this remains an area of active work to improve upon.

4.12. Halo model

The routines described in this subsection are implemented in `ccl_halomod.c`.

In this section we review a basic halo-model computation (Seljak 2000; Peacock & Smith 2000; Cooray & Sheth 2002) of the cross-correlation between any two cosmological fields and only requires knowledge of the halo profiles of the field in question. For example, in the case of the matter-density auto spectrum we need only know the halo density profiles. For the galaxy spectrum we require knowledge of the number of, and distribution of, galaxies as a function of halo mass. In this simple form the halo model is approximate and makes the assumption that haloes are *linearly* biased with respect to the *linear* matter field and also assumes that haloes are spherical with properties that are determined solely by the halo mass. It is possible to go beyond these simplified assumptions, and we direct the interested reader to Cooray & Sheth (2002); Smith et al. (2007); Giocoli et al. (2010); Smith & Markovic (2011).

The eventual aim for CCL is to have a halo model that can calculate the auto- and cross-spectra for any cosmological field combinations with parameters that can be taken either from numerical simulations or observational data. Currently we have only implemented the case of the matter-density auto spectrum, but we keep the notation as general as possible in the following:

Consider two 3D cosmological fields ρ_i and ρ_j , the cross power spectrum at a given redshift can be written as a sum of a two- and a one-halo term given by

$$P_{2H,ij}(k) = P_{\text{lin}}(k) \prod_{n=i,j} \left[\int_0^\infty b(M) \frac{dn}{dM} W_n(M, k) dM \right], \quad (50)$$

$$P_{1H,ij}(k) = \int_0^\infty \frac{dn}{dM} W_i(M, k) W_j(M, k) dM, \quad (51)$$

where M is the halo mass, dn/dM is the halo mass function defined as the first of equations (49) and $b(M)$ is the linear halo bias with respect to the linear matter density field, defined as the large-scale limit of the second of equations (49).

Equations (50) and (51) contain the (spherical) Fourier transform of the halo profile, or halo ‘window function’:

$$W_i(M, k) = \int_0^\infty 4\pi r^2 \frac{\sin(kr)}{kr} \rho_{H,i}(M, r) dr, \quad (52)$$

where $\rho_{H,i}(M, r)$ is the radial profile for the field i in a host halo of mass M . For example, if one is interested in matter fields then this would be the halo density profile, if one were interested in galaxies then this would be the number density and distribution of galaxies around a halo of mass M .

Note that the halo mass function and bias *must* satisfy the following properties for the total power spectrum to have the correct large-scale limit²⁰:

$$\frac{1}{\bar{\rho}_m} \int_0^\infty M \frac{dn}{dM} dM = 1 , \quad (53)$$

$$\frac{1}{\bar{\rho}_m} \int_0^\infty Mb(M) \frac{dn}{dM} dM = 1 . \quad (54)$$

If one uses a mass function and bias pair that are related via the peak-background split formalism (Mo & White 1996; Sheth et al. 2001), these conditions are automatically satisfied. In words these equations enforce that all matter is associated to a halo and that matter is on average unbiased with respect to itself. In the convention used in CCL the units of $P(k)$ will be exactly the units of $\rho_i \rho_j / \text{Mpc}^3$. The units of the W_i are those of ρ_i multiplied by volume.

For the matter power spectrum we use the halo profiles of Navarro, Frenk, & White (NFW; 1997):

$$\rho_H(M, r) \propto \frac{1}{r/r_s(1 + r/r_s)^2} , \quad (55)$$

which is written in terms of a scale radius r_s . The constant of proportionality fixed by the condition that the halo has total mass M when the boundary is set at the virial radius r_v , which is set such that the halo has a fixed density Δ_v with respect to the mean

$$M = 4\pi r_v^3 \Delta_v \bar{\rho} . \quad (56)$$

Finally, the scale radius is usually expressed in terms of the mass-dependent halo concentration parameter $c(M) = r_v/r_s$. We use the simple mass-concentration relation from Bullock et al. (2001)

$$c(M) = 9 \left(\frac{M}{M_*} \right)^{-0.13} , \quad (57)$$

where $\delta_c/\sigma(M_*) = 1$. Note that, in order to be consistent, one should use a value of Δ_v and $c(M)$ that is consistent with the halo definition used for the halo mass function and bias.

4.13. Photo- z implementation

The functionality described in this section is implemented in `ccl_lsst_specs.c`.

²⁰ Note that achieving these correct limits for some fields is difficult numerically because of the large amount of mass contained in low mass haloes according to most popular mass functions. Special care must be taken with the two-halo integral in the case of matter power spectra.

LSST galaxy redshifts will be obtained using photometry. A model is therefore required for the probability of measuring a photometric redshift z_{ph} for an object with hypothetical spectroscopic redshift z_{s} . CCL allows the user to flexibly provide their own photometric redshift model.

To take advantage of this functionality, the user writes a function which accepts as input a photometric redshift, a spectroscopic redshift, and a void pointer to a structure containing any further parameters of the photo-z model. This function will return the probability of measuring the input photometric redshift given the input spectroscopic redshift. Explicitly, it should take the form:

```
user_pz_probability(double z_ph, double z_s, void * user_par){...}
```

This function is responsible for extracting the photo-z model parameters from the void pointer `user_par` itself.

This model can be used when computing $\frac{dN^i}{dz}$ in photometric redshift bin i , as given by equation 60 below. An example of how the user can construct the required functions and structure can be found in `ccl_sample_run.c`. An example that uses a built-in Gaussian photo-z model is also provided.

4.14. LSST Specifications

CCL includes LSST specifications for the expected galaxy distributions of the full galaxy clustering sample and the lensing source galaxy sample. These enable the user to easily make forecasts for LSST. The functionality described in this section is implemented in `ccl_lsst_specs.c`.

The functional forms of the expected $\frac{dN}{dz}$ for clustering galaxies and lensing source galaxies are provided. Here, $\frac{dN}{dz}$ is the number density of galaxies as a function of true redshift.

In the case of lensing source galaxies, these forms are given in [Chang et al. \(2013\)](#), wherein three different cases are considered: fiducial, optimistic, and conservative. All three are included in CCL, and are indicated via a label of `DNDZ_WL_OPT`, `DNDZ_WL_FID`, and `DNDZ_WL_CONS` as appropriate. The functional form of $\frac{dN}{dz}$ for lensing source galaxies is given as:

$$\frac{dN}{dz} \propto z^\alpha \exp\left(-\frac{z^\beta}{z_0^\beta}\right). \quad (58)$$

The parameters, in the fiducial case, are given as $\alpha = 1.24$, $\beta = 1.01$, and $z_0 = 0.51$. In the optimistic case, this becomes $\alpha = 1.23$, $\beta = 1.05$, and $z_0 = 0.59$. The conservative case is given by $\alpha = 1.28$, $\beta = 0.97$, and $z_0 = 0.41$.

For the case of the clustering galaxy sample, the functional form is given by (LSST Science Collaboration 2009):

$$\frac{dN}{dz} \propto \frac{1}{2z_0} \left(\frac{z}{z_0} \right)^2 \exp \left(-\frac{z}{z_0} \right) \quad (59)$$

with $z_0 = 0.3$.

In order to be incorporated into forecasts or predictions, the above expressions for $\frac{dN}{dz}$ must be normalized, and the value of $\frac{dN}{dz}$ must be provided in a given photometric redshift bin. Support is provided for the user to input a flexible photometric redshift model, as described in Section 4.13. This takes the form of a function which returns the probability $p(z, z')$ of measuring a particular photometric redshift z , given a spectroscopic redshift z' and other relevant parameters. Also provided are functions to return σ_z at a given redshift for both lensing sources and clustering galaxies, for the case in which the user-defined function is a Gaussian photo- z model.

With this, $\frac{dN^i}{dz}$ of lensing or clustering galaxies in a particular photometric redshift bin i is given by:

$$\frac{dN^i}{dz} = \frac{\frac{dN}{dz} \int_{z_i}^{z_{i+1}} dz' p(z, z')}{\int_{z_{\min}}^{z_{\max}} dz \frac{dN}{dz} \int_{z_i}^{z_{i+1}} dz' p(z, z')} \quad (60)$$

where z_i and z_{i+1} are the photo- z edges of the bin in question.

Finally, the expected (linear, scale-independent) bias of galaxies in the clustering sample is also provided. It is given by (LSST Science Collaboration 2009):

$$b(z) = \frac{0.95}{D(z)} \quad (61)$$

where $D(z)$ is the linear growth rate of structure normalized to unity at $z=0$. Note that this bias definition requires the calculation of the linear growth rate and therefore is not yet supported for cosmologies with massive neutrinos.

5. Tests and validation

Our goal is for outputs of CCL to be validated against the results of a code-comparison project run within LSST-DESC down to a 10^{-4} or pre-established accuracy level if possible. In some cases, this level of accuracy is not necessary, as

Model	Ω_m	Ω_b	Ω_Λ	h_0	σ_8	n_s	w_0	w_a
flat LCDM	0.3	0.05	0.7	0.7	0.8	0.96	-1	0
w_0 LCDM	0.3	0.05	0.7	0.7	0.8	0.96	-0.9	0
w_a LCDM	0.3	0.05	0.7	0.7	0.8	0.96	-0.9	0.1
open w_a LCDM	0.3	0.05	0.65	0.7	0.8	0.96	-0.9	0.1
closed w_a LCDM	0.3	0.05	0.75	0.7	0.8	0.96	-0.9	0.1

Table 3. Cosmological models for the code comparison project.

other systematics which have not been considered in this version of CCL yet are expected to have a larger fractional impact. In the cases where this applies, we make it clear below.

A code comparison project was carried out among members of TJP where the following outputs of cosmological forecast codes were compared and validated:

1. growth factor at $z = 0, 1, 2, 3, 4, 5$,
2. comoving radial distance [Mpc/ h] at the same redshifts, as well as the corresponding distance moduli,
3. linear matter power spectrum, $P(k)$, from BBKS ([Bardeen et al. 1986](#)) in units of $(\text{Mpc}/h)^3$ at $z = 0, 2$ in the range $10^{-3} \leq k \leq 10h/\text{Mpc}$ with 10 bins per decade,
4. Eisenstein & Hu matter power spectrum in units of $(\text{Mpc}/h)^3$ at $z = 0$ in the range $10^{-3} \leq k \leq 10h/\text{Mpc}$ with 10 bins per decade, and
5. the mass variance at $z = 0$, $\sigma(M, z = 0)$ for $M = \{10^6, 10^8, 10^{10}, 10^{12}, 10^{14}, 10^{16}\} M_\odot/h$.

These predictions were produced and compared for different cosmologies, which are listed in the table below. The results agree to better than 0.1% relative accuracy for comoving distance and growth factor among all submissions, and for $P(k)$ and $\sigma(M)$ among codes which use the same BBKS conventions.

We noticed that there are 2 typos for the BBKS transfer function in “Modern Cosmology” ([Dodelson 2004](#)) compared to the original BBKS paper. The quadratic term should be $(16.1q)^2$ and the cubic term should be $(5.46q)^3$. The BBKS equation is correct in [Peacock \(1999\)](#). Using the wrong equation can give differences in the results above the 10^{-4} level.

From the comparison, we were also able to identify some typical issues which affect convergence at the desired level:

- For achieving 10^{-4} precision in $\sigma(M)$ and the normalisation of the power spectrum, one should check that the integral of σ_8 and $\sigma(M)$ has converged for the chosen values of $\{k_{\min}, k_{\max}\}$. After checking convergence, we achieved the desired precision.
- Also note that for $\sigma(M)$, it is important to set the desired precision level correctly for the numerical integrator. The integral usually yields $\sigma^2(M)$, and not $\sigma(M)$. Hence, one has to set the desired precision taking the exponent into account.
- The value of the gravitational constant, G , enters into the critical density. We found that failure to define G with sufficient precision would result in lack of convergence at the 10^{-4} level between the different submissions. Importantly, note that CAMB barely has 10^{-4} precision in G (and similarly, there might be other constants within CAMB/CLASS for which one should check the precision level). For CCL, we are using the value from the Particle Physics Handbook.
- Including/excluding radiation in the computation of the comoving distances and the growth function can easily make a difference of 10^{-4} at the redshifts required in this comparison.

In a second stage, we used the BBKS linear matter power spectrum from the previous step to compare two-point statistics for two redshift bins, resulting in three tomography combinations, $(1-1), (1-2), (2-2)$. We computed the following quantities:

- projected galaxy clustering tomography power spectra: density term only (no magnification, RSD, etc.) with non-evolving linear bias $b(z) = 1$, in the range $10 < \ell < 10000$, using 5 bins per decade,
- angular convergence tomography power spectra: leading order convergence term only (no magnification), in the same range and with the same resolution as the case above,
- angular galaxy clustering tomography correlation function, in the range $0.01 \text{ deg} < \theta < 5 \text{ deg}$, using 5 bins per decade, and
- angular shear tomography correlation functions (ξ_+, ξ_-) , similarly to above.

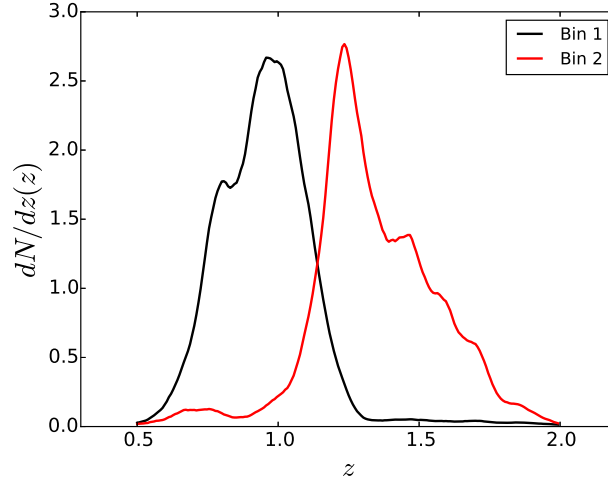


Figure 2. Binned redshift distributions used for code comparison project.

We adopted the following analytic redshift distributions: a Gaussian with $\sigma = 0.15$, centered at $z_1 = 1$; and another Gaussian with the same dispersion but centered at $z_2 = 1.5$. We repeated the exercise for two redshift distribution histograms shown in Figure 2.

In this second step, only 2 codes have been compared so far. More outputs are needed to guarantee convergence. Preliminarily, from these outputs, we have concluded that:

- The cross-correlation between bins is particularly sensitive to the number of points where the kernels have been sampled.
- The accuracy of the correlation function is sensitive to ℓ_{\max} . We had to use up to $\ell_{\max} = 3 \times 10^4$ for convergence (and we could not achieve 0.01% convergence).
- The large scales of the correlation function are sensitive to ℓ_{\min} . The use of the flat-sky approximation is also relevant on these scales.
- For sufficiently high precision, the correlation functions are sensitive to how the power spectrum is sampled and interpolated.

For C_ℓ computations, we required the relative difference between CCL and the benchmarks to be $< 10^{-3}$. We performed the test both for analytic redshift distributions and histograms.

To obtain realistic targets for the convergence of correlation function computations for LSST analyses, we calculate the expected statistical uncertainty of the clus-

tering and lensing correlation functions of the LSST gold sample (c.f. Sect. 4.14), assuming an effective source galaxy density of $n_{\text{eff}} = 26 \text{ gal/sq arcmin}$ for galaxy shape distortions, and galaxy density of $n_{\text{gold}} = 45 \text{ gal/sq arcmin}$ for number counts. Specifically, we calculate the Gaussian covariance of angular correlation functions following the formalism of [Joachimi et al. \(2008\)](#), and note that leaving out the non-Gaussian covariance terms makes this convergence criterion more conservative. We split the galaxy samples into 10 tomography bins, defined to contain equal numbers of galaxies. The accuracy test then proceeds as follows. We compared the difference between CCL calculated lensing and clustering correlations and the benchmarks for the analytic redshift distributions and for auto-correlations of redshift bins only. To pass the benchmark test, we required that this difference be smaller than half of the value of the errorbar derived from the covariance for each correlation function computed. Specifically, we take the value of the covariance in the bins centered at $z = 1$ and $z = 1.5$ to compare to the benchmarks.

The 3-dimensional correlation function $\xi(r)$ was validated by comparing with an independent, precise numerical transform. We calculated $\xi(r)$ by transforming the CCL non-linear Halofit power spectrum using this independent code for the five cosmologies listed in Table 3 at redshifts $z = 0, 1, 2, 3, 4, 5$. We then compared with the $\xi(r)$ from CCL with a sampling of $P(k)$ equal to `N_K_3DCOR` bins per decade. The default value of `N_K_3DCOR` = 100,000 results in a relative agreement at the level of $\Delta\xi(r)/\xi(r) < 2.5 \times 10^{-3}$ for $0.1 < r < 250$ Mpc and redshift zero. The agreement is better for higher redshifts. We also compared the absolute value of $r^2\xi(r)$ and find a maximum difference of $\Delta(r^2\xi(r)) < 3.0 \times 10^{-2}$ for the range $r = 0.1 - 250$ Mpc. This corresponds to approximately 0.08% of the BAO peak value of $r^2\xi(r)$. At the BAO peak, the difference is only 9.0×10^{-3} , or 0.024% of the peak height. The results are shown in Fig. 3 To further validate the $P(k) \rightarrow \xi(r)$ transform we performed a test using an analytical function $\xi(r) = (r/r_0)^a$, whose inverse transform $P(k)$ has a known analytic form. We used $r_0 = 5 \text{ Mpc}^{-1}$ and $a = -1.67$, which gives a rough approximation to the actual 3d correlation function. We then compared the CCL calculation of $\xi(r)$ to the known analytic result. The relative difference $\Delta\xi(r)/\xi(r)$ was found to be less than 0.3% in the range $2 < r < 250$ Mpc rising to about 5% at $r = 1000$ Mpc (see Fig. 4). For $r = 0.1 - 0.8$ Mpc the relative difference is $\approx 8\%$. The accuracy at low and high distances can be improved by increasing the range over which the power spectrum splines are evaluated.

Although this function approximates the true three-dimensional correlation distribution over the range of interest in r , the transform $P(k)$ does not have the correct behavior at low k where $P(k) \sim k$. Therefore, a second test was performed with the function $P(k) = Ak/(k_0 + k)^4$, where $A = 100$ and $k_0 = 0.045 \text{ Mpc}^{-1}$, that

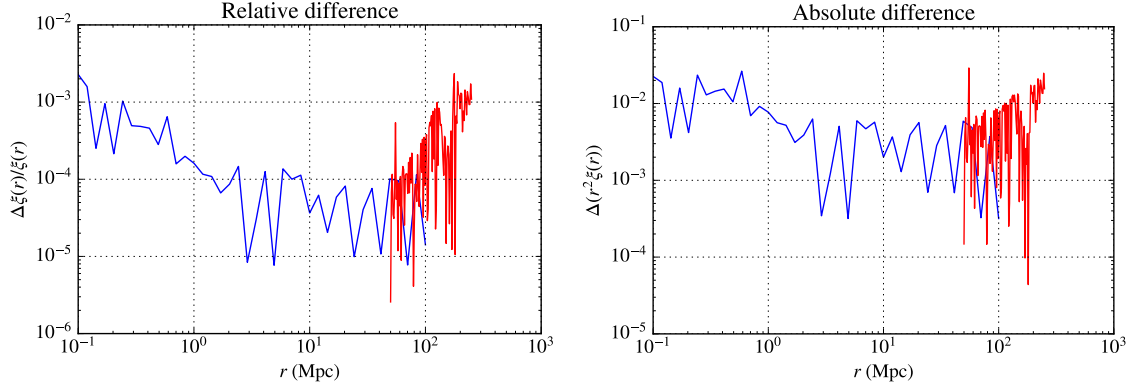


Figure 3. Comparison of the CCL calculation of the three-dimensional spatial correlation function $\xi(r)$ with a precise, numerical transform of the CCL non-linear Halofit power spectrum. The left panel shows the relative error $\Delta\xi(r)/\xi(r)$. The right panel shows the absolute error in $r^2\xi(r)$. Both panels are for the CCL1 model of Table ?? at redshift zero. The comparison made with 40 points in the range $r = 0.1 - 100$ Mpc (blue curve) and 100 points in the region $r = 50 - 250$ Mpc encompassing the the Baryon Acoustic Oscillation peak.

approximates the true behavior of the power spectrum for all k . The transform to $\xi(r)$ was performed using Mathematica and compared to the CCL calculation. The results, shown in Figure 4 show agreement to within 10^{-4} over most of the range in r . Since this power spectrum results in a correlation function that turns negative at $r \approx 150$ Mpc, the accuracy metric is large near this value.

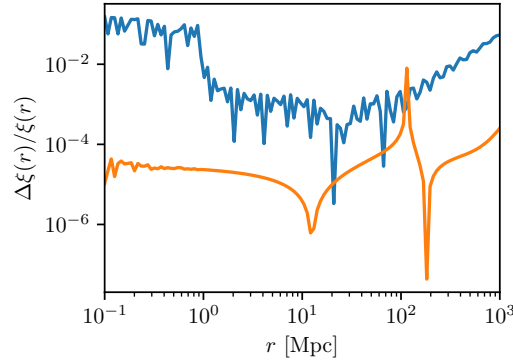


Figure 4. The relative error in the three-dimensional spatial correlation function computed using the CCL algorithm compared to an analytic function $\xi(r) = (r/r_0)^{1.67}$ (blue curve) and using $P(k) = Ak/(k_0 + k)^4$ (red dashed curve). Both functions have known analytic transforms, $\xi(r)$, but the second one has an asymptotic behavior that matches $P(k) \sim k$ at low k . In this validation test, the known $P(k)$ was transformed with the CCL algorithm and compared to the known analytic result for $\xi(r)$.

Additionally, independent codes were utilized to test the accuracy of halo mass function predictions. For the halo mass function, we compare the value of σ , $\log(\sigma^{-1})$, and the value of the halo mass function in the form used in [Tinker et al.](#)

(2008),

$$\log[(M^2/\bar{\rho}_m)dn/dM]. \quad (62)$$

We note that while we maintain the 10^{-4} for our evaluations of σ , the accuracy degrades to a value of 5×10^{-3} for the halo mass function evaluation, primarily at the high halo mass and high redshift domains. We find that this increased error is acceptable, as the level of precision is significantly better than the accuracy of current halo mass function models.

The implementation of the matter power spectrum emulation code from [Lawrence et al. \(2017\)](#) in CCL has been validated at first instance by comparing the direct output of the original code to CCL for the best fit cosmology (M000) in the range of wavenumbers spanned by the emulator predictions and confirming that the agreement is within the expectation from numerical errors (fractional difference of $< 10^{-5}$). We have also compared the CCL emulator outputs for certain cosmologies to smoothed power spectra from the simulations presented in [Lawrence et al. \(2017\)](#).²¹ The check ensures that the CCL outputs when calling the emulator are within 3% of the simulation benchmarks at $z = 0$ and for the k range of validity of the emulator. This essentially corresponds to a verification of the results presented in Figure 5 and Figure 6 of [Lawrence et al. \(2017\)](#).

In addition to the distance tests based on the TJP code comparison project described above, we include tests based on CLASS that cover the benchmark cosmologies listed in Table 3, as well as cosmologies with massive neutrinos. The agreement between CLASS and CCL on comoving radial distances and distance moduli is better than 10^{-6} . These tests are done at 10 logarithmically spaced redshifts between 0.01 and 1000. We also include tests of the growth factor for the same redshift range.

Finally, for cosmologies involving massive neutrinos, we have included also tests which compare comoving distance and distance modulus predictions from CCL from those produced by the `astropy` ([Astropy Collaboration et al. 2013](#)) library. In this case, we consider these comparison tests to pass if the agreement between the two predictions is 0.001 or better; this is due to the fact that `astropy` uses a fitting function for the neutrino phase-space integral while we compute the integral directly. The fitting function used by `astropy` is expected to match the true integral at approximately this level. As a sanity check, we also include a test which verifies that the power spectrum from CLASS as called via CCL matches that as called directly from CLASS in three test cosmologies with massive neutrinos.

²¹ Courtesy of Earl Lawrence and Katrin Heitmann.

CCL has a suite of test routines which, upon compilation, compare its outputs to the benchmarks from code comparison. These are run from the CCL root directory with the command `./build/check_ccl`.

6. Examples for C implementation

Examples of how to run CCL are provided in the `examples` sub-directory of the library. The first resource for a new user should be the `ccl_sample_run.c` file. This starts by setting up the CCL default configuration. Then, it creates the `cosmo` structure, which contains distances and power spectra splines, for example. There are example calls for routines that output comoving radial distances, the scale factor, the growth factor and σ_8 . Toy models are created for the redshift distributions of galaxies in the clustering and lensing samples, and for the bias of the clustering sample ($b(z) = 1 + z$). These are used for constructing the “tracer” structures via `CCL_Cltracer`, which can then be called to obtain the angular power spectra for clustering, cosmic shear and CMB lensing. All functions of redshift associated to each tracer can be retrieved at any arbitrary point using the same interpolation scheme used by CCL internally.

7. Python example

A Python wrapper for CCL is provided through a module called `pyccl`. The whole CCL interface can be accessed through regular Python functions and classes, with all of the computation happening in the background through the C code. The functions all support `numpy` arrays as inputs and outputs, with any loops being performed in the C code for speed.

The Python module has essentially the same functions as the C library, just presented in a more standard Python-like way. You can inspect the available functions and their arguments by using the built-in Python `help()` function, as with any Python module.

Below is a simple example Python script that creates a new `Cosmology` object, and then uses it to calculate the C_ℓ ’s for a simple lensing cross-correlation. It should take a few seconds on a typical laptop.

```
import pyccl as ccl
import numpy as np
```

```

# Create new Cosmology object with a given set of parameters. This keeps track
# of previously-computed cosmological functions
cosmo = ccl.Cosmology(Omega_c=0.27, Omega_b=0.045, h=0.67, A_s=2e-9, n_s=0.96)

# Define a simple binned galaxy number density curve as a function of redshift
z_n = np.linspace(0., 1., 200)
n = np.ones(z_n.shape)

# Create objects to represent tracers of the weak lensing signal with this
# number density (with has_intrinsic_alignment=False)
lens1 = ccl.WeakLensingTracer(cosmo, dndz=(z_n, n))
lens2 = ccl.WeakLensingTracer(cosmo, dndz=(z_n, n))

# Calculate the angular cross-spectrum of the two tracers as a function of ell
ell = np.arange(2, 10)
cls = ccl.angular_cl(cosmo, lens1, lens2, ell)
print cls

```

Further examples are collected in several Jupyter notebooks available in the `examples/` directory. These are:

Correlation.ipynb,
 Distance Calculations Example.ipynb,
 HMFexample.ipynb,
 Lensing angular power spectrum.ipynb,
 MCMC Likelihood Analysis.ipynb,
 Photo-z example.ipynb,
 Correlation_3d.ipynb,
 Power spectrum example.ipynb

Note that the likelihood analysis in the last notebook is not intended to be realistic, but it gives an operational example of how CCL can be integrated into such an anal-

ysis. In particular, the notebook only considers cosmic shear over one wide redshift bin and the covariance matrix adopted solely includes a contribution from cosmic variance. The “data vector” is simply a simulated using CCL theoretical predictions. For speed, theoretical predictions use the BBKS power spectrum implementation.

8. Technical notes on how the Python wrapper is implemented

The Python wrapper is built using the `swig` tool, which automatically scans the CCL C headers and builds a matching interface in Python. The default autogenerated `swig` interface can be accessed through the `pyccl.lib` module if necessary. A more user-friendly wrapper has been written on top of this to provide more structure to the module, allow `numpy` vectorization, and provide more natural Python objects to use (instead of opaque `swig`-generated objects).

The key parts of the wrapper are as follows:

setup.py—This instructs `swig` and other build tools on how to find the right source files and set compile-time variables correctly. Most of this information is provided by header files and SWIG interface files that are included through the `pyccl/ccl.i` interface file.

Note that certain compiler flags, like `-fopenmp`, are also set in `setup.py`. If you are not using `gcc`, you may need to modify these flags (see the `extra_compile_args` argument of the `setup()` function).

Interface (.i) files—These are kept in the `pyccl/` directory, and tell `swig` which functions to extract from the C headers. There are also commands in these files to generate basic function argument documentation, and remove the `ccl_` prefix from function names.

The interface files also contain code that tells `swig` how to convert C array arguments to `numpy` arrays. For certain functions, this code may also contain a simple loop to effectively vectorize the function.

The main interface file is `pyccl/ccl.i`, which imports all of the other interface files. Most of the CCL source files (e.g. `core.c`) have their own interface file too. For other files, mostly containing support/utility functions, `swig` only needs the C header (`.h`)

file to be specified in the main `ccl.i` file, however. (The C source file must also be added to the list in `setup.py` for it to be compiled successfully.)

Python module files—The structure of the Python module, as seen by the user, is organized through the `pyccl/__init__.py` file, which imports only the parts of the `swig` wrapper that are useful to the user. The complete autogenerated `swig` interface can be accessed through the `pyccl.lib` sub-module if necessary.

Individual sub-modules from CCL are wrapped in their own Python scripts (e.g. `power.py`), which typically provide a nicer “Pythonic” interface to the underlying CCL functions and objects. This includes automatically choosing whether to use the vectorized C function or not, as well as some conversions from Python objects to the autogenerated `swig` objects. Most of the core Python objects, like `Cosmology`, are defined in `core.py`. These objects also do some basic memory management, like calling the corresponding `ccl_free_*` C function when the Python object is destroyed.

Auto-generated wrapper files—The `swig` command is triggered when you run `setup.py`, and automatically generates a number of C and Python wrapper files in the `pyccl/` directory. These typically have names like `ccl*.c` and `ccl*.py`, and should not be edited directly, as `swig` will overwrite them when it next runs.

`pyccl/pyutils.py`—This file contains several generic helper functions for passing `numpy` arrays in and out of Python functions in a convenient way, and for performing error checking and some type conversions.

The build process will also create a `pyccl/ccllib.py` file, which is the raw autogenerated Python interface, and `_ccllib.so`, which is a C library containing all of the C functions and their Python bindings. A `build/` directory and `pyccl.egg-info/` directory will also be created in the same directory as `setup.py` when you compile `pyccl`. These (plus the `pyccl/_ccllib.so` file) should be removed if you want to do a clean recompilation. Running `python setup.py clean --all` will remove some, but not all, of the generated files.

9. Future functionality to be included

In the future, we hope that CCL will include other functionalities. Functionalities which are currently under development:

- further CMB observable predictions (beyond CMB lensing)²²,
- support for non-linear biasing models²³ (e.g. [McEwen et al. 2016](#)),
- halo density profiles²⁴,
- velocity correlation function²⁵,
- mass function emulators²⁶,
- and more power spectrum methods (see [4.8.9](#)).

10. Feedback

If you would like to provide feedback on CCL or contact the administrators, please do so through the CCL github repository located at <https://github.com/LSSTDESC/CCL>. We welcome users opening github issues.

11. Citing & using CCL

This software is a publicly released LSST DESC product which was developed within the LSST DESC using LSST DESC resources. DESC users should use it in accordance with the LSST DESC publication policy²⁷. External users are welcome to use the code outside DESC in accordance with the licensing information below.

This code has been released by DESC, although it is still under active development. It is accompanied by a journal paper that describes the development and validation of the library, which you can find in the `doc/ccl_paper` folder. You are welcome to re-use the code, which is open source and available under terms consistent with our LICENSE²⁸, which is a BSD 3-Clause²⁹ license.

For free use of the CLASS library, the CLASS developers require that the CLASS paper be cited: *CLASS II: Approximation schemes*, D. Blas, J. Lesgourgues, T. Tram, arXiv:1104.2933, JCAP 1107 (2011) 034. The CLASS repository can be found in <http://class-code.net>.

²² <https://github.com/LSSTDESC/CCL/issues/428>

²³ <https://github.com/LSSTDESC/CCL/pull/444>

²⁴ <https://github.com/LSSTDESC/CCL/issues/407>

²⁵ <https://github.com/LSSTDESC/CCL/issues/429>

²⁶ <https://github.com/LSSTDESC/CCL/issues/235>

²⁷ <http://lsstdesc.org/Collaborators>

²⁸ <https://github.com/LSSTDESC/CCL/blob/master/LICENSE>

²⁹ <https://opensource.org/licenses/BSD-3-Clause>

12. License

Copyright ©2016-2018, the LSST DESC CCL contributors (<https://github.com/LSSTDESC/CCL/graphs/contributors>). The repository can be found at <https://github.com/LSSTDESC/CCL>. All rights reserved.

Redistribution and use in source and binary forms, with or without modification, are permitted provided that the following conditions are met:

- Redistributions of source code must retain the above copyright notice, this list of conditions and the following disclaimer.
- Redistributions in binary form must reproduce the above copyright notice, this list of conditions and the following disclaimer in the documentation and/or other materials provided with the distribution.
- Neither the name of CCL (<https://github.com/LSSTDESC/CCL>) nor the names of its contributors may be used to endorse or promote products derived from this software without specific prior written permission.

THIS SOFTWARE IS PROVIDED BY THE COPYRIGHT HOLDERS AND CONTRIBUTORS “AS IS” AND ANY EXPRESS OR IMPLIED WARRANTIES, INCLUDING, BUT NOT LIMITED TO, THE IMPLIED WARRANTIES OF MERCHANTABILITY AND FITNESS FOR A PARTICULAR PURPOSE ARE DISCLAIMED. IN NO EVENT SHALL THE COPYRIGHT HOLDER OR CONTRIBUTORS BE LIABLE FOR ANY DIRECT, INDIRECT, INCIDENTAL, SPECIAL, EXEMPLARY, OR CONSEQUENTIAL DAMAGES (INCLUDING, BUT NOT LIMITED TO, PROCUREMENT OF SUBSTITUTE GOODS OR SERVICES; LOSS OF USE, DATA, OR PROFITS; OR BUSINESS INTERRUPTION) HOWEVER CAUSED AND ON ANY THEORY OF LIABILITY, WHETHER IN CONTRACT, STRICT LIABILITY, OR TORT (INCLUDING NEGLIGENCE OR OTHERWISE) ARISING IN ANY WAY OUT OF THE USE OF THIS SOFTWARE, EVEN IF ADVISED OF THE POSSIBILITY OF SUCH DAMAGE.

We would like to thank the organisers of the the DESC collaboration meetings at: Oxford (July 2016), SLAC (March 2016), and ANL (2015), and the LSST-DESC Hack Week organisers (CMU, November 2016), where this work was partly developed. We would also like to acknowledge the contribution of the participants of the TJP Code Comparison Project, some of whom are among the CCL contributors, for providing the benchmarks for testing CCL. Finally, we are grateful for the

feedback received from other working groups of DESC, including Strong Lensing, Supernovae and Photometric Redshifts.

Author contributions are listed below.

Husni Almoubayyed: wrote an mcmc jupyter notebook example, reviewed code/contributed to issues.

David Alonso: Co-led project; developed structure for angular power spectra; implemented autotools; integrated into LSS pipeline; contributed to: background, power spectrum, mass function, documentation and benchmarks; reviewed code

Jonathan Blazek: Planning capabilities and structure; documentation and testing.

Philip Bull: Implemented the Python wrapper and wrote documentation for it; general bug fixes, maintenance, and code review; enhanced the installer and error handling system.

Jean-Éric Campagne: Angpow builder and contributed to the interface with CCL.

N. Elisa Chisari: Co-led project, coordinated hack projects & communication, contributed to: correlation function & power spectrum implementation, documentation, and comparisons with benchmarks.

Alex Drlica-Wagner: Helped with document preparation.

Zilong Du: Implemented the 3d correlation function.

Tim Eifler: Reviewed/tested code.

John Ellison: Implemented the 3d correlation function; wrote text describing 3d correlation function for this note.

Renée Hlozek: Contributed initial code for error handling structures, reviewed other code edits.

Mustapha Ishak: Contributed to planning of code capabilities and structure; reviewed code; identified and fixed bugs.

Shahab Joudaki: Created physical density function and documentation.

Matthew Kirby: Performed comparison of physical constants.

David Kirkby: Writing, testing and reviewing code. Asking questions.

Elisabeth Krause: Initiated and co-led project; developed CLASS interface and error handling; contributed to other code; reviewed pull requests.

Francois Lanusse: Worked on install procedure

C. Danielle Leonard: Wrote and tested code for LSST specifications, user-defined photo-z interface, and support of massive neutrinos; reviewed other code; wrote text for this note.

Christiane S. Lorenz: Contributed to accurate high-redshift cosmological background quantities and benchmarked background splines.

Phil Marshall: Helped with document preparation.

Thomas McClintock: Wrote Python documentation.

Sean McLaughlin: Wrote doxygen documentation and fixed bugs/added functionality to distances.

Alexander Mead: Wrote halo model code

Jérémy Neveu: Contributed to Angpow and built the interface with CCL.

Stéphane Plaszczynski: Contributed to Angpow and contributed to the interface with CCL.

Javier Sanchez: Modified setup.py to allow pip installation and uninstall.

Sukhdeep Singh: Contributed to the correlation functions code.

Anže Slosar: Wrote and reviewed code.

Tilman Tröster: Wrote code for user-changable precision parameters, added distance and growth factor tests, found and fixed bugs.

Antonio Villarreal: Contributed to initial benchmarking, halo mass function code, and general code and issues review.

Michal Vrátil: Wrote documentation and example code, reviewed code.

Joe Zuntz: Wrote initial infrastructure, C testing setup, and reviewed code.

References

- Alonso, D., Bull, P., Ferreira, P. G., Maartens, R., & Santos, M. G. 2015, *ApJ*, 814, 145
- Angulo, R. E., Springel, V., White, S. D. M., et al. 2012, *MNRAS*, 426, 2046
- Astropy Collaboration, Robitaille, T. P., Tollerud, E. J., et al. 2013, *A&A*, 558, A33
- Bardeen, J. M., Bond, J. R., Kaiser, N., & Szalay, A. S. 1986, *ApJ*, 304, 15
- Bartelmann, M., & Schneider, P. 2001, *PhR*, 340, 291
- Blas, D., Lesgourgues, J., & Tram, T. 2011, CLASS: Cosmic Linear Anisotropy Solving System, Astrophysics Source Code Library, ascl:1106.020
- Bonvin, C., & Durrer, R. 2011, *PhRvD*, 84, 063505
- Bullock, J. S., Kolatt, T. S., Sigad, Y., et al. 2001, *MNRAS*, 321, 559
- Campagne, J.-E., Neveu, J., & Plaszczynski, S. 2017, *ArXiv e-prints*, arXiv:1701.03592
- Challinor, A., & Lewis, A. 2011, *PhRvD*, 84, 043516
- Chang, C., Jarvis, M., Jain, B., et al. 2013, *Monthly Notices of the Royal Astronomical Society*, 434, 2121
- Chevallier, M., & Polarski, D. 2001, *International Journal of Modern Physics D*, 10, 213
- Cooray, A., & Sheth, R. 2002, *Physics Reports*, 372, 1
- Dodelson, S. 2004, *Modern Cosmology*, Vol. 57, 60–61, doi:10.1063/1.1784308
- Durrer, R. 2008, *The Cosmic Microwave Background* (Cambridge University Press)
- Eisenstein, D. J., & Hu, W. 1998, *ApJ*, 496, 605
- Giocoli, C., Bartelmann, M., Sheth, R. K., & Cacciato, M. 2010, *MNRAS*, 408, 300
- Hamilton, A. J. S. 2000, *MNRAS*, 312, 257
- Hirata, C. M., Mandelbaum, R., Ishak, M., et al. 2007, *MNRAS*, 381, 1197
- Hirata, C. M., & Seljak, U. 2004, *PhRvD*, 70, 063526
- Joachimi, B., & Bridle, S. L. 2010, *A&A*, 523, A1
- Joachimi, B., Schneider, P., & Eifler, T. 2008, *A&A*, 477, 43
- Kamionkowski, M., & Spergel, D. N. 1994, *ApJ*, 432, 7
- Lattanzi, M., & Gerbino, M. 2017, *ArXiv e-prints*, arXiv:1712.07109

- Lawrence, E., Heitmann, K., Kwan, J., et al. 2017, *ApJ*, 847, 50
- Lesgourgues, J., & Pastor, S. 2012, *ArXiv e-prints*, arXiv:1212.6154
- Linder, E. V. 2003, *Physical Review Letters*, 90, 091301
- LSST Science Collaboration. 2009, *ArXiv e-prints*, arXiv:0912.0201
- Mamajek, E. E., Prsa, A., Torres, G., et al. 2015, *ArXiv e-prints*, arXiv:1510.07674
- Mangano, G., Miele, G., Pastor, S., et al. 2005, *Nuclear Physics B*, 729, 221
- McEwen, J. E., Fang, X., Hirata, C. M., & Blazek, J. A. 2016, *JCAP*, 9, 015
- Mo, H. J., & White, S. D. M. 1996, *MNRAS*, 282, 347
- Mohr, P. J., Newell, D. B., & Taylor, B. N. 2016, *Reviews of Modern Physics*, 88, 035009
- Navarro, J. F., Frenk, C. S., & White, S. D. M. 1997, *ApJ*, 490, 493
- Peacock, J. A. 1999, *Cosmological Physics*, 704
- Peacock, J. A., & Smith, R. E. 2000, *MNRAS*, 318, 1144
- Schneider, A., & Teyssier, R. 2015, *JCAP*, 12, 049
- Seljak, U. 2000, *MNRAS*, 318, 203
- Sheth, R. K., Mo, H. J., & Tormen, G. 2001, *MNRAS*, 323, 1
- Smith, R. E., & Markovic, K. 2011, *PhRvD*, 84, 063507
- Smith, R. E., Scoccimarro, R., & Sheth, R. K. 2007, *PhRvD*, 75, 063512
- Takahashi, R., Sato, M., Nishimichi, T., Taruya, A., & Oguri, M. 2012, *ApJ*, 761, 152
- Talman, J. 2009, *Computer Physics Communications*, 180, 332
- Tinker, J., Kravtsov, A. V., Klypin, A., et al. 2008, *ApJ*, 688, 709
- Tinker, J. L., Robertson, B. E., Kravtsov, A. V., et al. 2010, *ApJ*, 724, 878
- Watson, W. A., Iliev, I. T., D'Aloisio, A., et al. 2013, *MNRAS*, 433, 1230
- Yoo, J. 2010, *PhRvD*, 82, 083508
- Yoo, J., Fitzpatrick, A. L., & Zaldarriaga, M. 2009, *PhRvD*, 80, 083514